CHAPTER 1

INTRODUCTION

1.1 THE TRANSISTOR

Transistor is the fundamental building block of modern electronic devices, and is found everywhere in modern electronic systems. It was development in 1947 by John Bardeen, Walter Brattain, and William Shockley and thus was revolutionized the field of electronics, and paved the way for smaller and cheaper radios, calculators, and computers among other things. The inventors of transistors were jointly awarded the 1956 Nobel Prize in Physics for their achievement. Transistor is a semiconductor device used to amplify and switch electronic signals and electrical power. It is composed of semiconductor material with at least three terminals for connection to an external circuit. A voltage or current applied to one pair of the transistor's terminals changes the current through another pair of terminals. Because the controlled (output) power can be higher than the controlling (input) power, a transistor can amplify a signal. Transistors have become the key ingredient of all digital circuits, including computers. Today's microprocessors contain tens of millions of microscopic transistors. Some transistors are packaged individually, but many more are found embedded in integrated circuits.

1.1.1 Brief history of transistor

Bell Laboratories, one of the world's largest industrial laboratories, was the research arm of the giant telephone company American Telephone and Telegraph (AT&T). In 1945, Bell Labs was beginning to look for a solution to a long-standing problem. AT&T brought its former president, Theodore Vail, out of retirement to help it fight off competition erupting from the expiration of Alexander Graham Bell's telephone patents.

Vail's solution: transcontinental telephone service. In 1906, the eccentric American inventor Lee De Forest developed a triode in a vacuum tube. It was a device that could amplify signals, including, it was hoped, signals on telephone lines as they were transferred across the country from one switch box to another. AT&T bought De Forest's patent and vastly improved the tube. It allowed the signal to be amplified regularly along the line, meaning that a telephone conversation could go on across any distance as long as there were amplifiers along the way. But the vacuum tubes that made that amplification possible were extremely unreliable, used too much power and produced too much heat. In the 1930s, Bell Lab's director of research, Mervin Kelly, recognized that a better device was needed for the telephone business to continue to grow. He felt that the answer might lie in a strange class of materials called semiconductors. After the end of World War II, Kelly put together a team of scientists to develop a solid-state semiconductor switch to replace the problematic vacuum tube. The team would use some of the advances in semiconductor research during the war that had made radar possible. A young, brilliant theoretician, Bill Shockley, was selected as the team leader. [18] Shockley drafted Bell Lab's Walter Brattain, an experimental physicist who could build or fix just about anything, and hired theoretical physicist John Bardeen from the University of Minnesota. Shockley filled out his team with an eclectic mix of physicists, chemists and engineers. The group was diverse, yet close knit. Walter Brown, a physicist who joined the group in 1951, recalls hearing about exuberant parties and good lunches. Betty Sparks, Shockley's secretary, recalled the group's high spirits at her wedding to Morgan Sparks. They called their lab "Hell's Bells Laboratory."

In the spring of 1945, Shockley designed what he hoped would be the first semiconductor amplifier, relying on something called the "field effect." His device was a small cylinder coated thinly with silicon, mounted close to a small, metal plate. It was, as University of Illinois Electrical Engineer Nick Holonyak said, a crazy idea. Indeed, the device didn't work, and Shockley assigned Bardeen and Brattain to find out why. According to author Joel Shurkin, the two largely worked unsupervised; Shockley spent most of his time working alone at home. Ensconced in Bell Labs' Murray Hill facilities,

Bardeen and Brattain began a great partnership. Bardeen, the theoretician, suggested experiments and interpreted the results, while Brattain built and ran the experiments. Technician Phil Foy recalls that as time went on with little success, tensions began to build within the lab group. In the fall of 1947, author Lillian Hoddeson says, Brattain decided to try dunking the entire apparatus into a tub of water. Surprisingly, it worked a little bit. Brattain began to experiment with gold on germanium, eliminating the liquid layer on the theory that it was slowing down the device. It didn't work, but the team kept experimenting using that design as a starting point. Shortly before Christmas, Bardeen had an historic insight.

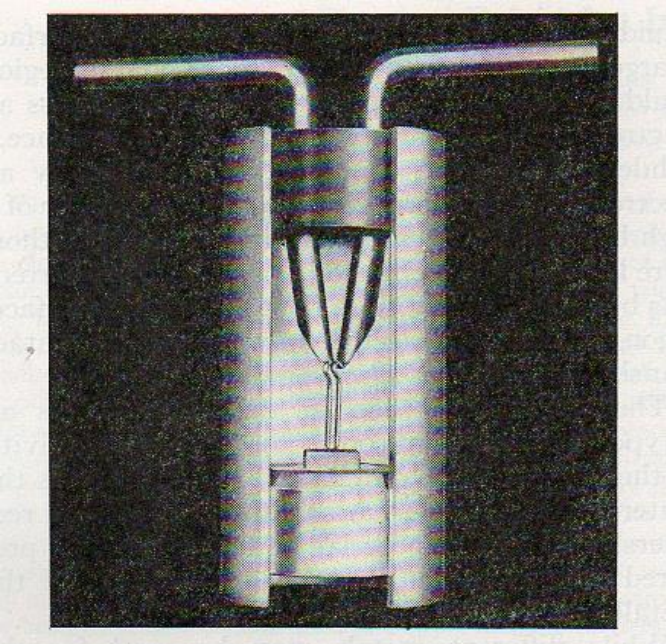

Figure 1.1: Microphotograph of a cutaway model of a transistor

Everyone thought they knew how electrons behaved in crystals, but Bardeen discovered they were wrong. The electrons formed a barrier on the surface. His breakthrough was what they needed. Without telling Shockley about the changes they were making to the investigation, Bardeen and Brattain worked on. On December 16, 1947, they built the point-contact transistor, made from strips of gold foil on a plastic triangle, pushed down into contact with a slab of germanium. When Bardeen and Brattain called

Shockley to tell him of the invention, Shockley was both pleased at the group's results and furious that he had not been directly involved. He decided that to preserve his standing, he would have to do Bardeen and Brattain one better. His device, the junction (sandwich) transistor, was developed in a burst of creativity and anger, mostly in a hotel room in Chicago. It took him a total of four weeks of working pen on paper, although it took another two years before he could actually build one. His device was more rugged and more practical than Bardeen and Brattain's point-contact transistor, and much easier to manufacture. It became the central artifact of the electronic age.

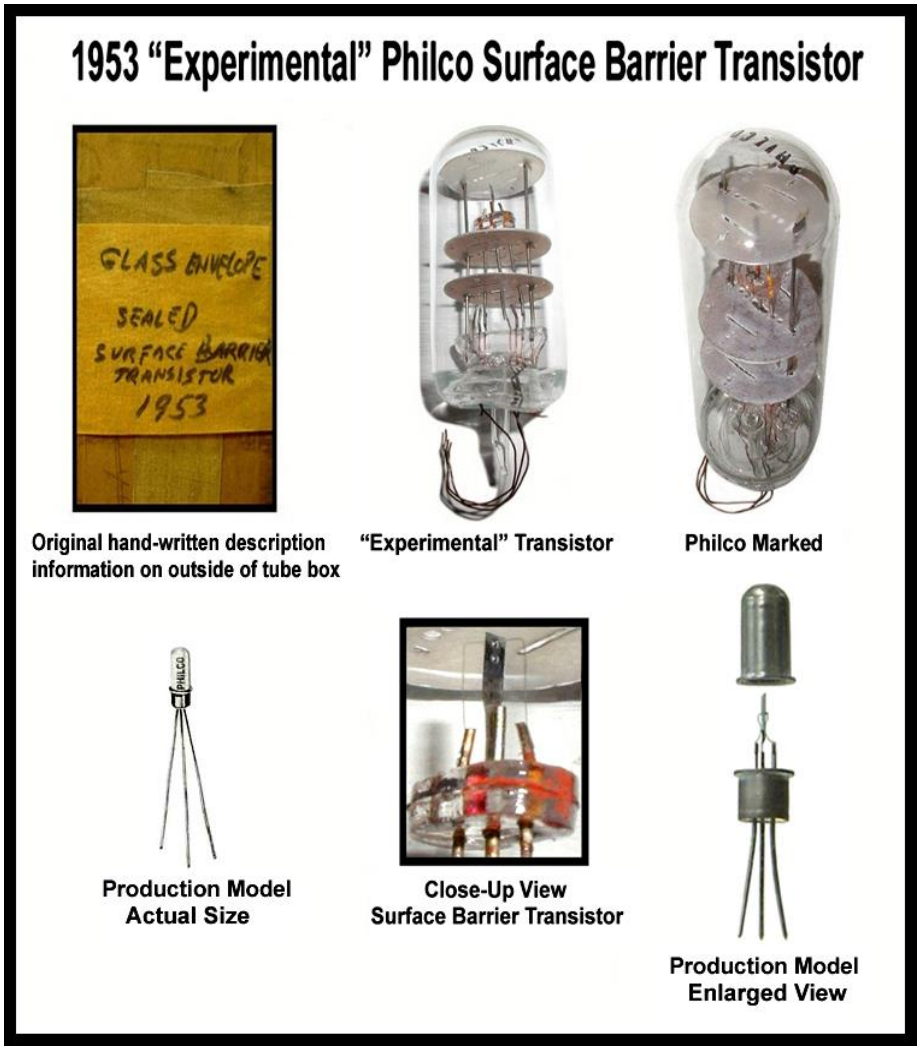

Figure 1.2: Experimental transistor (1953)

The term “transistor” was coined by John R. Pierce tailoring the words “transfer” & “resistor”. According to physicist/historian Robert Arns, legal papers from the Bell Labs patent show that William Shockley and Gerald Pearson had built operational versions from Lilienfeld's patents, yet they never referenced this work in any of their research papers or historical articles [19].Bardeen, Brattain and Shockley were awarded the Nobel Prize in physics in 1956. The first silicon transistor was produced by Texas Instruments in 1954. This was the work of Gordon Teal, an expert in growing crystals of high purity, who had previously worked at Bell Labs. The first MOS transistor actually built was by Kahng and Atalla at Bell Labs in 1960 [20].

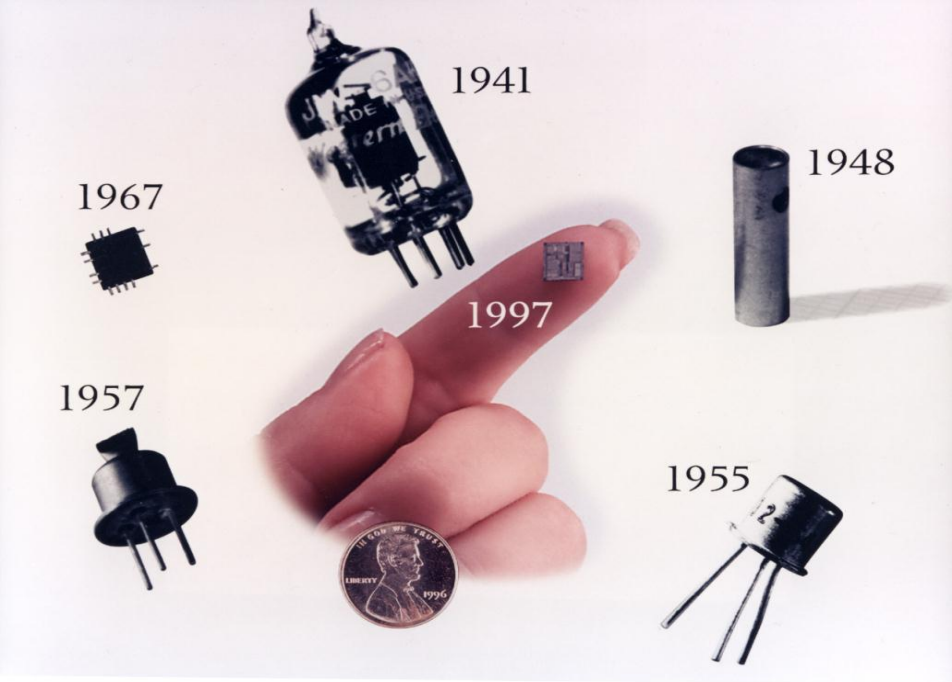

Figure 1.3: Transistor and Integrated Circuits (ICs) chronology [Source: Bell Labs].

1.1.2 Category of transistors

After the success of Bell Labs, many other organizations came ahead and invested hugely in the research of solid-state electronics. Various forms of transistors have been modeled, patented and experimented. A few of them are categorized here in the following table.

Table 1.1: Different type of Transistors (adapted from [21])

Criteria	**Subdivision**	**Category**
Structure	Junction Transistor (Bipolar Transistor)	BJT (Bipolar Junction Transistor) HBT (Heterojunction Bipolar Transistor) Insulated Gate Bipolar Transistor (IGBT)
	Field Effect Transistor (Unipolar Transistor)	Junction Field Effect Transistor (JFET) Metal Oxide Semiconductor FET (MOSFET or IGFET)
Polarity		BJT: npn, pnp
		FET: n-channel, p-channel
Material		Germanium (Ge), Silicon (Si), Gallium Arsenide (GaAs), Indium Phosphide (InP), Silicon Carbide (SiC) etc
Power rating		Low, medium, high
Frequency		Radio frequency (RF),microwave etc.
Application		Switch, audio, high voltage, super-beta, etc.
Packaging		Through hole metal or plastic, surface mount etc.

1.2 THE BIPOLAR TRANSISTOR

A bipolar junction transistor (BJT or bipolar transistor) is a type of transistor that relies on the contact of two types of semiconductor for its operation. BJTs can be used as amplifiers, switches, or in oscillators. BJTs can be found either as individual discrete components, or in large numbers as parts of integrated circuits. Bipolar transistors are so named because their operation involves both electrons and holes. These two kinds of charge carriers are characteristic of the two kinds of doped semiconductor material. In contrast, unipolar transistors such as the field-effect transistors have only one kind of charge carrier. Charge flow in a BJT is due to bidirectional diffusion of charge carriers across a junction between two regions of different charge concentrations. A bipolar transistor essentially consists of a pair of PN junction diodes that are joined back to back. The regions of a BJT are called emitter; collector and base .A discrete transistor has three leads for connection to these regions. By design, most of the BJT collector current is due to the flow of charges injected from a high-concentration emitter into the base where there are minority carriers that diffuse toward the collector, and so BJTs are classified as minority-carrier devices.

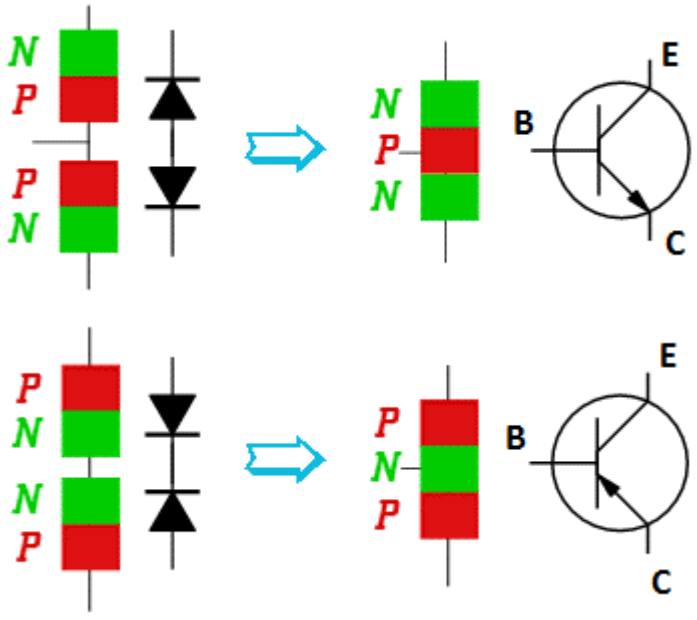

Figure 1.4: Schematic symbols for PNP- and NPN- type BJTs

A bipolar transistor takes shape as the doping of a semiconductor proceeds. The process of adding controlled impurities into the crystal lattice of a semiconductor is known as doping. The amount of impurity (dopant) added to an intrinsic semiconductor varies its level of conductivity. Doped semiconductors are often referred to as extrinsic. By adding impurity to intrinsic semiconductors, the electrical conductivity may be varied not only by the number of impurity atoms but also, by the type of impurity atom and the changes may be thousand folds and million folds. For example- 1 cm^3 of a metal or semiconductor specimen has a number of atoms on the order of 10^{22}. Since every atom in metal donates at least one free electron for conduction in metal, 1 cm3 of metal contains free electrons on the order of 10^{22}. At the temperature close to 20 °C, 1 cm^3 of intrinsic germanium contains about 4.2×10^{22} atoms and 2.5×10^{13} free electrons & 2.5×10^{13} holes. The addition of 0.001% of arsenic donates an extra 10^{17} free electrons in the same volume and the electrical conductivity increases about 10,000 times [22].

1.2.1 The dopants

Dopants are classified as either electron acceptors or donors. A donor atom donates weakly-bound valence electrons to the material, creating excess negative charge carriers. These weakly-bound electrons can move about in the crystal lattice relatively freely and can facilitate conduction in the presence of an electric field. Conversely, an activated acceptor produces a hole. Semiconductors doped with donor impurities are called *n*-type, while those doped with acceptor impurities are known as *p*-type. The *n* and *p* type designations indicate which charge carrier acts as the material's majority carrier. The opposite carrier is called the minority carrier, which exists due to thermal excitation at a much lower concentration compared to the majority carrier.

The number of dopant atoms needed to create a difference in the ability of a semiconductor to conduct is very small. When a comparatively small number of dopant atoms are added on the order of one per 100 million atoms, the doping is said to be low or light. When many more dopant atoms are added on the order of one per ten thousand

atoms, the doping is referred to as heavy or high. This is often mentioned as *n*+ for *n*-type doping or *p*+ for *p*-type doping. When a semiconductor is doped to such high level, it acts almost like a conductor and is referred as a degenerate semiconductor [22].

1.2.2 The doping process

Some dopants are added as (usually) the gallium arsenide boule is grown using the Bridgeman technique or the Czochralski process, giving each wafer an almost uniform initial doping. For desired device properties, selected areas typically controlled by photolithography are further doped by such processes as diffusion and ion implantation. The latter method being more popular in large production runs because of increased controllability. The molecular beam epitaxy (MBE) or chemical vapor deposition (CVD) technologies are also used in transistor manufacturing where precisely controlled doping is required [29].

1.2.3 n^+-p-n transistor operation

An n-p-n transistor essentially consists of a pair of PN junction diodes that are joined back-to-back. This forms a sort of a sandwich where one kind of semiconductor is placed in between two others. The thin common region is called base. Metal contacts are made to all three regions. The operation of a bipolar junction transistor depends on the forward and the reverse current of the two back-to-back *p*-*n* junctions. The forward-biased junction, which injects electrons into the center *p* region, is called base-emitter junction and the reversed-biased junction, which collects the injected electrons, is called the base-collector junction. The region, which serves as the source of injected electrons, is called the emitter and the *n* region into which electrons are swept by the reverse-biased junction is called the collector. The center region is called the base.

The construction and terminal voltages for and NPN transistor is shown in Fig. 1.5. The voltage between the Base and Emitter (V_{BE}) is positive at the Base and negative at the Emitter because for an NPN transistor, the Base terminal is always positive with respect to the Emitter. Also the collector supply voltage positive with respect to Emitter (V_{CE}).

So for an NPN transistor to conduct the collector is always more positive with respect to both the Base and the Emitter.

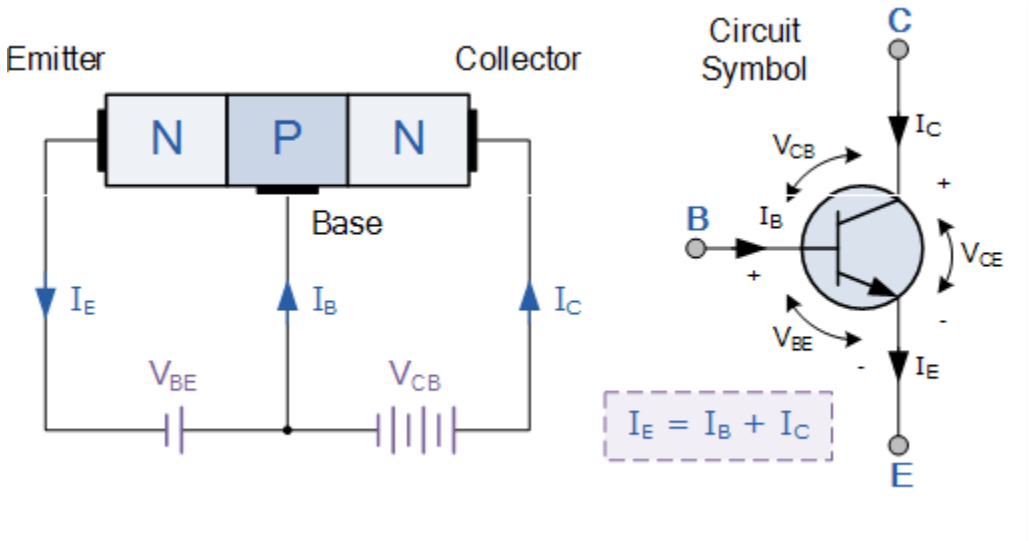

Figure 1.5: The schematic diagram of an n^+-p-n bipolar junction transistor. Conventional direction of current flow is assumed.

Then the voltage sources are connected to an NPN transistor as shown in Fig. 1.6. The Collector is connected to the supply voltage V_{CC} via the load resistor, RL which also acts to limit the maximum current flowing through the device. The Base supply voltage V_B is connected to the Base resistor R_B, which again is used to limit the maximum Base current.

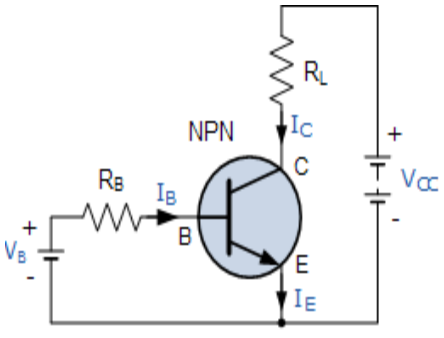

Figure 1.6: NPN transistor connection

We know that the transistor is a "current" operated device (Beta model) and that a large current (I_C) flows freely through the device between the collector and the emitter terminals when the transistor is switched "fully-ON". However, this only happens when a small biasing current (I_B) is flowing into the base terminal of the transistor at the same time thus allowing the Base to act as a sort of current control input.

The transistor current in an NPN transistor is the ratio of these two currents (I_c/I_b), called the DC Current Gain of the device and is given the symbol Beta (β). The value of β can be large up to 200 for standard transistors, and it is this large ratio between I_C and I_B that makes the NPN transistor a useful amplifying device when used in its active region as I_B provides the input and I_C provides the output. Note that β has no units as it is a ratio. Also, the current gain of the transistor from the Collector terminal to the Emitter terminal, I_C/I_E, is called Alpha (α), and is a function of the transistor itself (electrons diffusing across the junction). As the emitter current I_E is the sum of a very small base current plus a very large collector current, the value of alpha α, is very close to unity, and for a typical low-power signal transistor this value ranges from about 0.950 to 0.999.

To have a good n^+-p-n transistor, it is preferred that almost all the electrons injected by the emitter into the base be collected. Thus the p-type base region should be narrow. This requirement is summed up by specifying neutral base width should be less than the diffusion length of electron in the base. With this requirement satisfied, an average electron injected at the emitter junction will diffuse to the depletion region of the base-collector junction without recombination in the base. A second requirement is that the emitter current (I_E) crossing the emitter junction should be composed almost entirely of electrons injected into the base rather than holes crossing from base to emitter [23].

1.2.4 Advantages of bipolar transistor

Bipolar devices can switch signals at high speeds, and can be manufactured to handle large currents so that they can serve as high-power amplifiers in audio equipment and in wireless transmitters. Bipolar devices are not especially effective for weak-signal amplification, or for applications requiring high circuit impedance. It operates in medium to high Voltage range. It has high current density and low forward voltage drop. Although Complementary Metal Oxide Semiconductor (CMOS) transistor has acquired an ever-increasing role, the bipolar transistor retains its position as a technology of choice for high-speed circuits, ultra-high-frequency discrete logic circuits such as emitter coupled logic (ECL), power amplifiers in cellular phones, mixed-signal & precision analog components, microwave power amplifiers and in other applications like fiber-optic communication. The speed advantage (higher frequencies) together with trans-conductance (gm), high current gain (β) and low $1/f$ noise continue to make the bipolar transistor the device of choice for many demanding applications [24]. One of the important figures of merit of BJTs is the transition frequency f_T, presently which ranges in the GHz level [2.5] and the maximum oscillation frequency f_{max} which also ranges in the same level is another important high frequency parameter.

1.3 HETEROJUNCTION BIPOLAR TRANSISTOR

Heterojunction bipolar transistor (HBT) differs from the traditional homojunction bipolar transistor (BJT) in that at least one of two junctions is formed between dissimilar semiconductor materials. As a result, the energy band-gap as well as all other material properties can be different in the emitter, base and collector. Moreover, a gradual change or "grading" of the material is possible within each region. Heterojunction bipolar transistors are not just an added complication. On the contrary, the use of heterojunctions provides an additional degree of freedom, which can result in vastly improved devices compared to the homojunction counterparts.

A typical flat band diagram of an HBT and the energy band diagram under forward active bias is presented in figure 1.7.

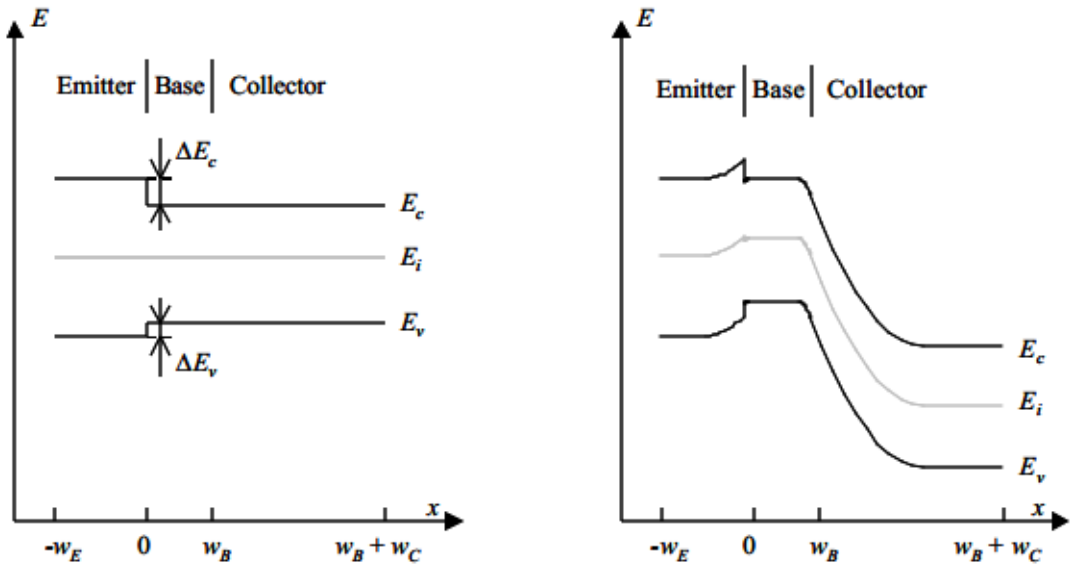

(a) (b)

Figure 1.7: (a) Flat band diagram of an HBT (b) Energy band diagram under forward active bias

With two hetero junctions, a bipolar transistor is identified as double heterojunction bipolar transistor (DHBT) or simply HBT. With one homojunction and another heterojunction, a bipolar transistor is termed as single heterojunction bipolar transistor (SHBT). Typically the emitter of the SHBT is wide bandgap material which allows heavy doping of the base for reduced base resistance while the emitter is more lightly doped reducing the capacitance and improving the high frequency performance. In the DHBT, the collector and emitter have wide bandgap materials allowing the same advantages of the SHBT, with the additional improvement of increased breakdown voltage and decreased minority carrier injection from the base to the collector in saturation mode [25].

Different types of elements and compound semiconductor materials are used to fabricate heterojunction. HBTs are named after the materials used in substrate or in the epitaxial layers. Properties of material used determine the characteristics of HBTs and their costs. Table 1.2 shows a list of such common materials used to fabricate HBTs of different genres.

Table 1.2: Examples of material combination frequently used to form HBTs (The devices are grouped according to their substrate material) [26]

Type	Emitter	Base	Collector	Substrate
SHBT	AlGaAs	GaAs	GaAs	GaAs
SHBT	GaInP	GaAs	GaAs	
DHBT	GaAs	InGaAs	GaAs	
SHBT	InP	GaInAs	GaInAs	InP
SHBT	AlInAs	GaInAs	GaInAs	
DHBT	AlInAs	GaInAs	InP	
SHBT	α-Si	Si	Si	Si
SHBT	SiC	Si	Si	
DHBT	Si	SiGe	Si	

The HBT improves on the BJT in that it can handle signals of very high frequencies, up to several hundred GHz. It is commonly used in modern ultrafast circuits, mostly radio-frequency (RF) systems, and in applications requiring high power efficiency, such as RF power amplifiers in cellular phones. The idea of employing a heterojunction is as old as the conventional BJT, dating back to a patent from 1951 [27]. The principal difference between the BJT and HBT is in the use of differing semiconductor materials for the emitter-base junction and the base-collector junction, creating a heterojunction. The effect is to limit the injection of holes from the base into the emitter region, since the

potential barrier in the valence band is higher than in the conduction band. Unlike BJT technology, this allows a high doping density to be used in the base, reducing the base resistance while maintaining gain. The efficiency of the heterojunction is measured by the Kroemer factor [28] named after Herbert Kroemer who was awarded a Nobel Prize for his work in this field in 2000.

HBT has low base spreading resistance, high electron mobility (for compound semiconductors), Low 1/f noise and ballistic and overshoot effects. It can be integrated with HEMTs, MESFETs, Schottky diodes. In comparison with BJTs, HBTs show better performance in terms of emitter injection efficiency, base-emitter capacitance, base resistance and cut-off frequency.

1.3.1 The InGaAs device physics

Indium gallium arsenide (InGaAs), also called gallium indium arsenide, is a common name for a family of chemical compounds of three chemical elements, indium, gallium, and arsenic. Indium and gallium are both boron group elements, often called "group III", while arsenic is a pnictogen or “group V" element. In semiconductor physics, compounds of elements in these groups are often called "III-V" compounds. Because they belong to the same group, indium and gallium play similar roles in chemical bonding, and InGaAs is often regarded as an alloy of gallium arsenide and indium arsenide, with its properties being intermediate between the two and depending on the proportion of gallium to indium. Under typical conditions, InGaAs is a semiconductor, and it is especially significant in optoelectronics technology, InGaAs is a direct band gap, pseudo-binary alloy composed of two III-V semiconducting materials: $(GaAs)_X$ and $(InAs)_{1-X}$. The alloy is miscible over the entire compositional range from GaAs (band gap = 1.42 eV at 300 K) to InAs (band gap = 0.34 eV at 300 K. $In_{1-x}Ga_xAs$ is a technologically important semiconductor widely exploited in photovoltaic, sensor and laser applications.

The behaviour of a semiconductor junction depends crucially on the alignment of the energy bands at the interface. Semiconductor interfaces can be organized into three

types of heterojunctions: straddling gap (type I), staggered gap (type II) or broken gap (type III) as seen in the figure 1.8

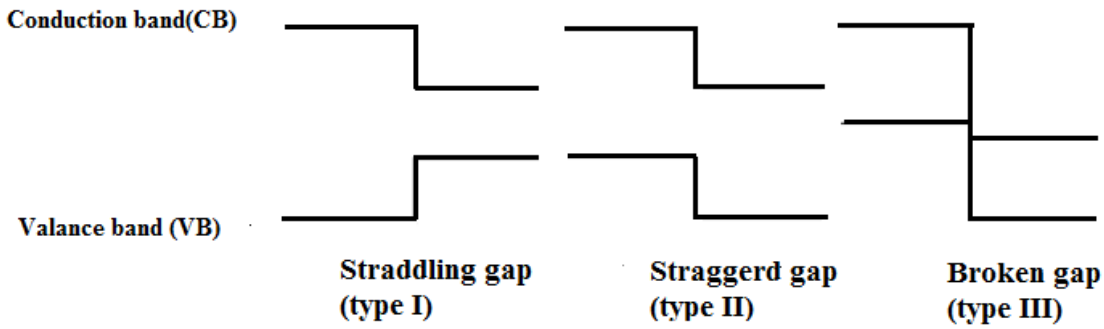

Figure 1.8: The three types of semiconductor heterojunctions organized by band alignment.

Indium Gallium arsenide has a lattice parameter that increases linearly with the concentration of InAs in the alloy. The liquid-solid phase diagram shows that during solidification from a solution containing GaAs and InAs, GaAs is taken up at a much higher rate than InAs, depleting the solution of GaAs. During growth from solution, the composition of first material to solidify is rich in GaAs while the last material to solidify is richer in InAs. This feature has been exploited to produce ingots of InGaAs with graded composition along the length of the ingot. However, the strain introduced by the changing lattice constant causes the ingot to be polycrystalline, and limiting the characterization to a few parameters, with uncertainty due to the continuous compositional grading in the materials.

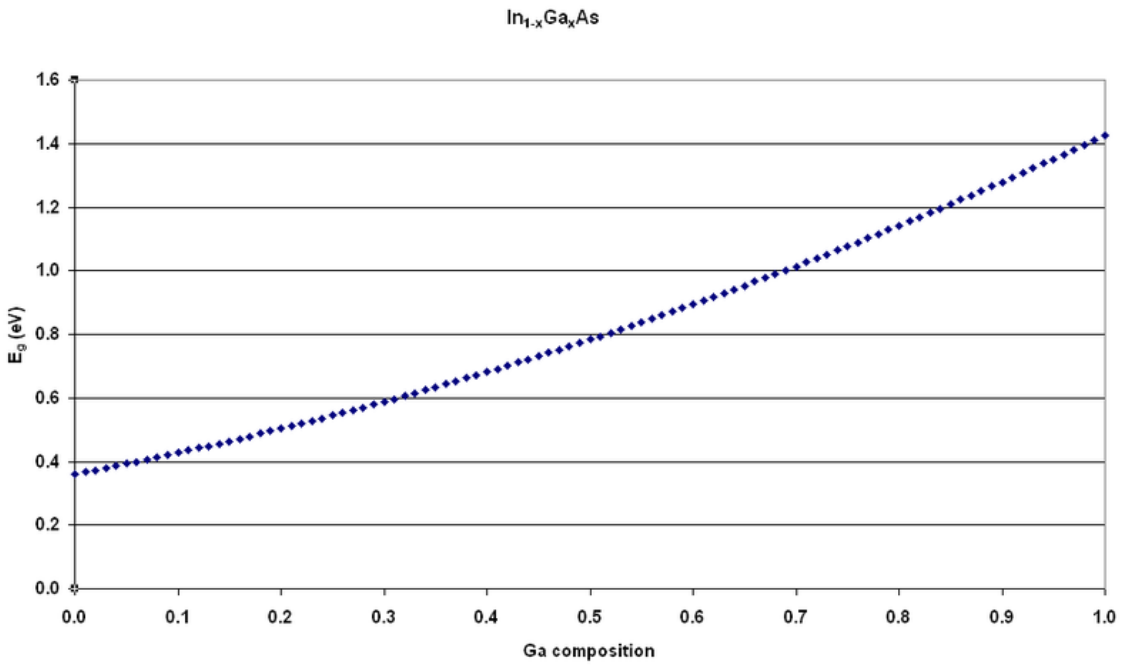

Figure 1.9: Energy gap versus gallium compostion for InGaAs

J.C. Woolley and his students at the University of Ottawa used this approach in the 1960s to characterise the optical properties of a large number of III-V pseudo binary alloy systems. Although the polycrystalline nature of the samples used made them unsuitable for device applications, the experimental results and analysis do provide a comprehensive overview of the potential of III-V semiconductor alloys. While more precise measurements have been obtained on single-crystal samples, such as the case of epitaxial InGaAs grown lattice-matched on InP, Woolley's results represent the best body of data today for alloy compositions that cannot by synthesized as single-crystal epitaxial films for lack of the appropriate substrate.

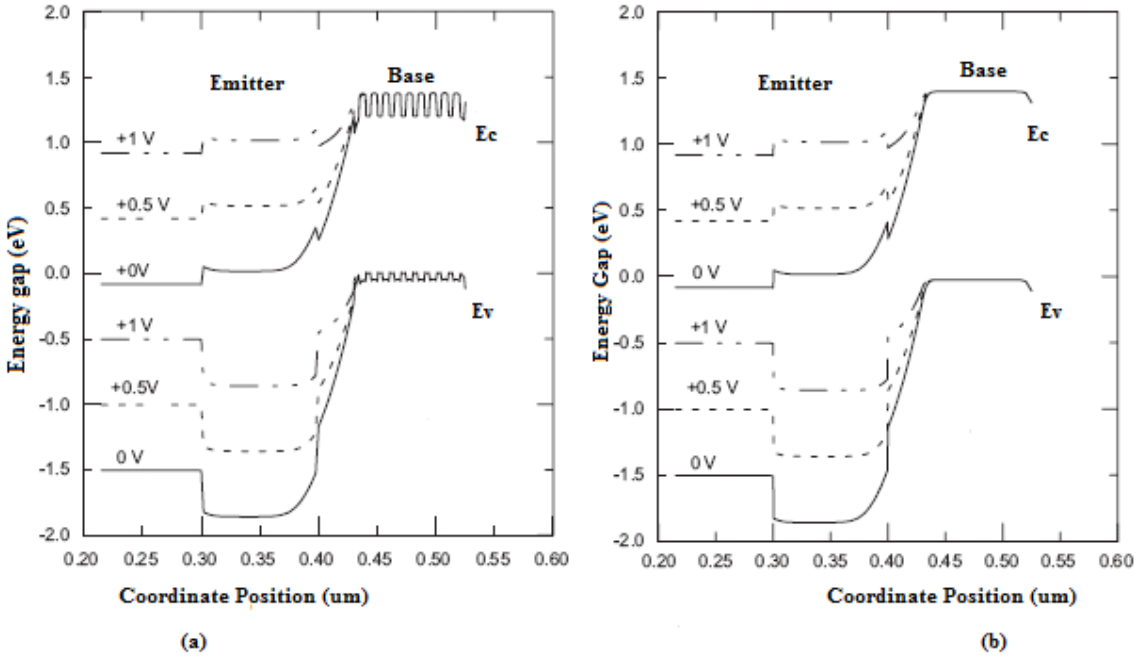

Figure 1.10: InGaAs/GaAs HBT (a) with superlattice-base structure (b) without superlattice-base structure

As emitter-base potential barrier is reduced in the InGaAs HBT with respect to the GaAs BJT, thereby allowing increased electron injection from emitter to base. The enhanced electron injection leads to a higher collector current and current gain.InGaAs exhibits higher collector current (J_C) and approximately the same base current (J_B) like the GaAs BJT. The increase in J_C for the InGaAs HBT in turn leads to an increase in current gain (β). The current gain depends linearly on the band offset due to In (Indium) grading across the base an exponentially on the In induced band offset at the EB junction. Therefore, β is dependent on the In profile shape and can be modified for particular circuit applications. The introduction of In in the base in effects decouples β from the base doping. This fact implies that the base doping can be increased without degrading β. Note that higher base doping reduces the base resistance which has positive implications in terms of frequency response and broadband noise.

1.3.2 The InGaAs HBT

The amount of indium in the base is graded in InGaAs graded heterojuncttion transistors, making the ban gap narrower at the collector than the emitter. Field-assisted transport in the base generates by tapering of the band gap, which speeds transport through the base and increases frequency response.

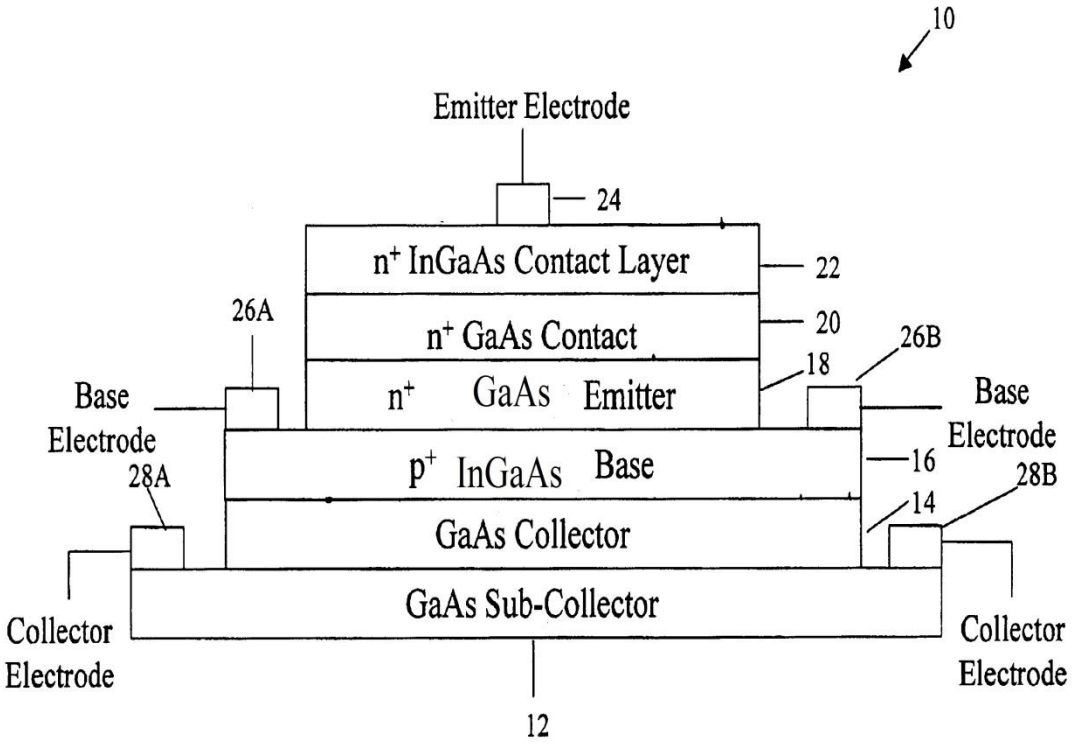

Figure 1.11: The schematic diagram showing the cross section of a InGaAs heterojunction bipolar transistor.

The InGaAs HBTs have better device performance parameters (β, gm ad f_T) compared to gallium arsenide. They satisfy the requirement of RF circuits such as modems, mixers, voltage controlled oscillator (VCOs), power amplifiers etc; mixed signal circuits like fractional N synthesizes and analog to digital converters and in the precision analog circuit such as op-amps, band gap references, temperature bias control and current

mirrors etc. Further band gap engineering of InGaAs facilities in reducing forward voltage drop of the emitter-base junction by uniform grading at the emitter-base junction without effecting the other parameters which makes it a best candidate for low voltage applications in wireless phones and other low power battery operated products, in addition to allowing very complex custom designs, high speed and high breakdown voltage InGaAs HBTs can be merged with high density CMOS using a mixed signal methology.

A summary of the advantages of InGaAs technology over other technologies is given below:

- Size and power consumption are critical for mobile applications. For a given f_T, a InGaAs HBT would require only about a third of the collector current as compared to a GaAs BJT [34]. MOSFETs have lower g_m *per* mA as compared to BJT/HBT and the current required to obtain the same f_T for MOSFETs is larger [35].

- Breakdown voltages of InGaAs HBTs are about twice those of GaAs for same f_T. As far as RF CMOS technology is concerned, the breakdown voltage as well as the maximum operating voltage is limited due to thin oxide breakdown and hot-carrier effects [36].

- HBTs have better noise performance since they have higher β and f_T as compared to BJTs. The base resistance of a InGaAs HBT is lower than the GaAs. CMOS devices have higher minimum noise figure as compared to bipolar devices when biased at the same current density [37].

- By optimizing the In profile in the base of a InGaAs HBT, much higher Early voltage can be obtained than in BJTs. This results in higher *ro* which maximizes gain and also helps in improving stability. The short-channel RF-MOSFETs have much lower ro than InGaAs HBTs due to increased channel-length modulation effects.

- HBTs have higher current gain than conventional BJTs as a result of which improved linearization by feedback is possible. Cancellation of the base-emitter heterojunction capacitance improves the inter-modulation performance of HBT as compared to MESFET and HEMT. This results in excellent linearity data as reported in [38].

- Due to the advantages of InGaAs HBT, such as higher current gain, early voltage, breakdown voltage and transit frequency, reduced base resistance as well as better transport properties of the base, performance approaching GaAs technologies can be achieved. Moreover, InGaAs technology is currently being used to develop electronics for space applications due to their excellent analog and radio frequency performance over an extremely wide range of temperatures [39]. Therefore InGaAs technology is a very good choice for high frequency and high temperature electronics at a competitive cost.

1.3.3 Applications of InGaAs HBT

Heterojunction manufacturing generally requires the use of molecular beam epitaxy (MBE) or chemical vapor deposition (CVD) technologies in order to precisely control the deposition thickness and create a cleanly lattice-matched abrupt interface. MBE and CVD tend to be very complex and expensive compared to traditional indium device fabrication.

Despite their expense, heterojunctions have found use in a variety of specialized applications where their unique characteristics are critical:

- **Lasers:** Using heterojunctions in lasers was first proposed in 1963 when Herbert Kroemer, a prominent scientist in this field, suggested that population inversion could be greatly enhanced by heterostructures. By incorporating a smaller direct band gap material like GaAs between two larger band gap layers

like InAs, carriers can be confined so that lasing can occur at room temperature with low threshold currents. It took many years for the material science of heterostructure fabrication to catch up with Kroemer's ideas but now it is the industry standard. It was later discovered that the band gap could be controlled by taking advantage of the quantum size effects in quantum well heterostructures. Furthermore, heterostructures can be used as waveguides to the index step which occurs at the interface, another major advantage to their use in semiconductor lasers. Semiconductor diode lasers used in CD and DVD players and fiber optic transceivers are manufactured using alternating layers of various III-V and II-VI compound semiconductors to form lasing heterostructures.

- **Bipolar transistors:** When InGaAs heterojunction is used as the base-emitter junction of a bipolar junction transistor, extremely high forward gain and low reverse gain result. This translates into very good high frequency operation (values in tens to hundreds of GHz) and low leakage currents. This device is called InGaAs heterojunction bipolar transistor (HBT).
- **Field effect transistors:** InGaAs heterojunctions are used in high electron mobility transistors (HEMT) which can operate at significantly higher frequencies (over 500 GHz). The proper doping profile and band alignment gives rise to extremely high electron mobility by creating a two dimensional electron gas within a dopant free region where very little scattering can occur.
- Recent advances in heterojunction bipolar transistor (HBT) technology enable trial uses in some systems utilizing advantages of HBTs such as high power handling capability, high current drive capability, low $1/f$ noise characteristics, with high frequency and high speed performance

CHAPTER 2

BACKGROUND OF WORK

2.1 THE EARLY VOLTAGE AND COMMON EMITTER CURRENT GAIN

Depletion layer widths of bipolar junction transistor (BJT) and the quasi-neutral regions vary as the voltages applied to the base-emitter and base-collector junctions are changed. This causes the collector current to vary with the collector-emitter voltage as illustrated in Figure 2.1

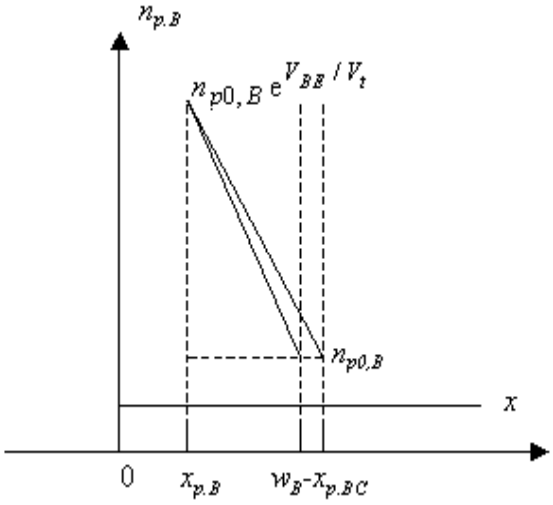

Figure 2.1: Variation of the minority-carrier distribution in the base quasi-neutral region due to a variation of the base-collector voltage.

A variation of the base-collector voltage results in a variation of the quasi-neutral width in the base. The gradient of the minority-carrier density in the base therefore changes, yielding an increased collector current as the collector-base current is increased. This effect is referred to as the Early effect. The Early effect is observed as an increase in the collector current with increasing collector-emitter voltage as illustrated with Figure 2.2

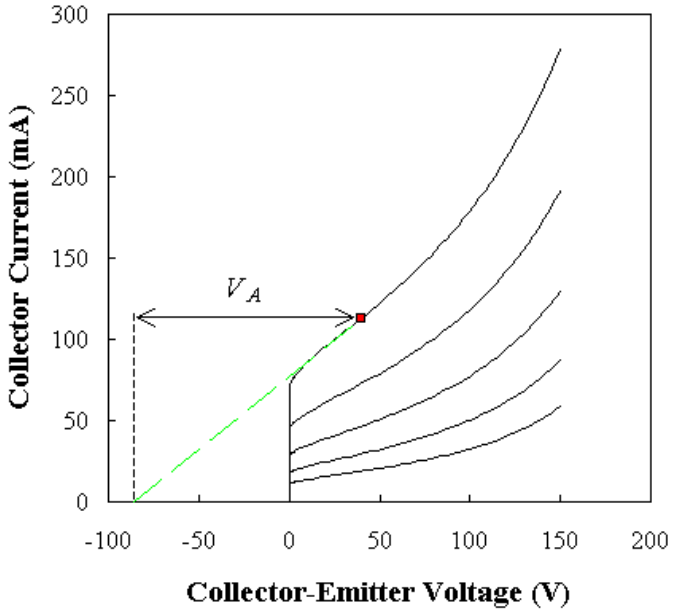

Figure 2.2: Collector current increase with an increase of the collector-emitter voltage due to the Early effect. The Early voltage, V_A, is also indicated on the figure.

So the Early effect is the variation in the width of the base in a bipolar junction transistor (BJT) due to a variation in the applied base-to-collector voltage, named after its discoverer James M. Early. A greater reverse bias across the collector–base junction, for example, increases the collector–base depletion width, decreasing the width of the charge neutral portion of the base. The collector depletion region also increases under reverse bias, more than does that of the base, because the collector is less heavily doped. The principle governing these two widths is charge neutrality. The narrowing of the collector does not have a significant effect as the collector is much longer than the base. The emitter–base junction is unchanged because the emitter–base voltage is the same

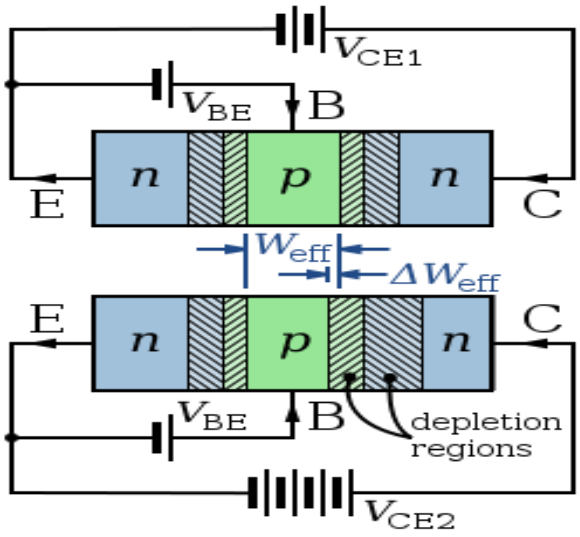

Figure 2.3: The neutral (i.e. active) base is green, and the depleted base regions are hashed light green. The neutral emitter and collector regions are dark blue and the depleted regions hashed light blue. Under increased collector–base reverse bias, the lower panel of Figure 1 shows a widening of the depletion region in the base and the associated narrowing of the neutral base region.

Base-narrowing has two consequences that affect the current:

- There is a lesser chance for recombination within the "smaller" base region.
- (b) The charge gradient is increased across the base, and consequently, the current of minority carriers injected across the emitter junction increases.

Both these factors increase the collector or "output" current of the transistor with an increase in the collector voltage. This increased current is shown in Figure 2.2. The Early voltage, V_A, is obtained by drawing a line tangential to the transistor *I-V* characteristic at the point of interest. The Early voltage equals the horizontal distance between the point chosen on the *I-V* characteristics and the intersection between the tangential line and the horizontal axis. It is indicated on the figure by the horizontal arrow.

In the forward active region the Early effect modifies the collector current (I_C) and the forward common-emitter current gain (β_F) as typically described by the following equations [1]-[2].

$$I_C = I_S\left(1 + \frac{V_{CE}}{V_A}\right)e^{\frac{V_{BE}}{V_T}}$$

$$\beta_F = \beta_{FO}\left(1 + \frac{V_{CE}}{V_A}\right)e^{\frac{V_{BE}}{V_T}}$$

Where

- V_{CE} is the collector–emitter voltage
- V_T is the thermal voltage $\frac{KT}{q}$
- $V_A$is the Early voltage
- β_{FO} is forward common-emitter current gain at zero bias.

Some models base the collector current correction factor on the collector–base voltage V_{CB} (as described in base-width modulation) instead of the collector–emitter voltage V_{CE} [3].Using V_{CB} may be more physically plausible, in agreement with the physical origin of the effect, which is a widening of the collector–base depletion layer that depends on V_{CB}.

The Early effect can be accounted for in small-signal circuit models (such as the hybrid-pi model) as a resistor defined as [4]

$$r_O = \frac{V_A + V_{CE}}{I_C} \approx \frac{V_A}{I_C}$$

in parallel with the collector–emitter junction of the transistor. This resistor can thus account for the finite output resistance of a simple current mirror or an actively loaded common-emitter amplifier.

2.2 THE IMPORTANCE OF EARLY VOLTAGE AND CURRENT GAIN

Several recent works have been reported on the Early voltage and current gain. The Early voltage describes the output conductance and the load drive capability bipolar transistors so high early voltage is desirable for any device. The Early effect has been studied extensively in conventional bipolar junction transistor (BJTs).The Heterojunction Bipolar Transistor (HBT) was developed to overcome the limitations of conventional bipolar transistors. In a classical homojunction bipolar transistor the base width must be reduced to achieve high speed (the transit time of the minority carriers through the base is proportional to the square of the base width).However, if the width of the base is reduced, the base resistance is increased, which slows the device response time. The base resistance can be reduced by increasing the base doping concentration, but then the injection into emitter decreases the current gain. It is, therefore, impossible to optimize the base thickness (width) and doping concentration for high-speed, high gain and low base resistance. The use of heterojunctions, however, permits improved transit time, current gain and base resistance simultaneously.

2.3 REVIEW OF RECENT WORKS ON EARLY VOLTAGE AND CURRENT GAIN

The effect of surface recombination of AlGaAs/GaAs/ AlGaAs HBT on the V_A was studied by Chiu et al.[5]. This model did not consider the effect of electric field on mobility while calculating V_A. Effect of Ge content at the collector base junction on V_A was investigated by Dong et al.[6]. At high doping concentration and high Ge content, neutral base recombination effect on β were analysed by Ningyue et al. for uniform base doping profile [7]. Prinz et al. studied V_A and β in HBT where band gap varies across the base [8]. This model is applicable for uniformly doped base and the effect of velocity saturation and field dependent diffusivity were neglected in this model. Yuan et al. modified Prinz's works by including neutral base re-combination effect on V_A [9]. Early voltage improvement using deep sub-micron technique was proposed by Conrad et al [10]. Modelling and improvement of current gain for a uniform doped base SiC power

bipolar junction transistor was done by Domeij [11].A new bipolar junction transistor for enhanced current gain and reduced hot carrier degradation was proposed by Kumar et al. [12]. Ge content in the base as well as heavy base doping cause BGN [13]. So BGN due to heavy doping should con-sider while calculating V_A and β. Zareba derived a new model of V_A considering field dependent diffusivity, velocity saturation and band gap narrowing effects for Gaussian doped base HBT[14]. This model was not in closed form and it was done only for triangular germanium profile in the base. Babcock et al. have done a comprehensive investigation of temperature dependence of current gain (β) and Early voltage (V_A) for SiGe-*npn* transistors [15]. Babcock et al. also done comprehensive investigation of Early voltage (V_A) versus drive current dependence for SiGe-pnp bipolar transistors fabricated on thick-film SOI [16]. Ziao B. et al. generalized SGP model of standard Early voltage for SiGe- *npn* heterojunction bipolar transistors (HBTs) [17]. A complete closed form analytical model of V_A and β for GaAs/InGaAs/GaAs HBT with different base doping profile (uniform and exponential) and trapezoidal/triangular/box indium profile in the base is yet to be reported where the necessary effects were considered.

2.4 SCOPE OF DISSERTAION

The primary objectives of this research are given below.

- To observe the effects of base doping profile and Indium profile on V_A and β.
- To correlate how these two parameters are dependent on diffusion coefficient, effective intrinsic carrier concentration and electric field.
- To derive analytical model for V_A and β for uniform and exponential base doping profile with arbitrary Indium profiles heterojunction bipolar transistor (HBT).
- Field dependent mobility, doping dependent mobility, band gap narrowing (BGN) (due to both heavy doping and presence of Indium Gallium Arsenide content in the base) and velocity saturation effects considering in this model.

2.5 LAYOUT OF THE CHAPTERS

In chapter one importance of early voltage and current gain have been discussed and recent works on V_A and β have been reviewed and the justification of carrying out the research is given. In chapter two InGaAs device physics and basic equations for diffusivity, electric field, collector current density and Early voltage were derived which were used to make close form analytical model for Early voltage and current gain in the next chapters. In chapter three details mathematical analysis were provided to derive closed form of Early voltage and common emitter current gai for uniform and exponential base doping profiles and arbitrary Indium profile. In chapter four graphical representation of Early voltage, current gain, cut –off frequency, intrinsic carrier concentration, diffusivity were studied with respect to various parameters variation. Also the results obtained by using our models were compared with the results available in the previous research works. Finally in chapter five possible future of studies were discussed.

2.6 DERIVATION OF MAIN EQUATIONS

Collector current density, Early voltage and electric field equations were derived in this chapter which will be used in the next chapters for the derivation of Early voltage and current gain closed from model. Collector current equation was derived from the basic equation of drift and diffusion part of current density. It was derived by using boundary conditions for base-emitter and base-collector current junction carried density. Early voltage equation was derived from its basic form and using collector current equation. Electric field equation was derived in the same way. All these equations derived in this chapter is used in Chapter 3 by considering various influences to make closed form of Early voltage and common emitter current gain.

2.6.1 Derivation of collector current density (JCO) and common emitter current gain (β)

The electron current density J_n for an arbitrary base doping concentration NB(x) for InGaAs can be derived by using general transport equation provided by Van Overstraeten [30].

$$J_n = qD_{nInGaAs}(x)\frac{d_{nieInGaAs}(x)}{dx} + q\mu_{nInGaAs}(x)n_{ieInGaAs}(x)E_{InGaAs}(x) \qquad (2.1)$$

Where electric field equation is [31]

$$E_{InGaAs}(x) = \frac{kT}{q}\left(\frac{1}{p(x)}\frac{dp(x)}{dx} - \frac{1}{n^2_{ieInGaAs}(x)}\frac{dn^2_{ieInGaAs}(x)}{dx}\right) \qquad (2.2)$$

Equation (2.1) contains two parts, one is diffusion part and another is drift part. Diffusion part is dependent on gradient of electron concentration and drift part is dependent on electric field.

Where q is the charge ofelectron, $D_{nInGaAs}$ is the diffusion coefficient, $\mu_{nInGaAs}$,the mobility, $n_{ieInGaAs}$ the effective intrinsic carrier concentration for InGaAs HBT.

The boundary condition at the emitter-base junction is [32]

$$n(0) = \frac{n^2_{ie}(0)}{N_B(0)}\exp\left(\frac{qV_{EB}}{KT}\right) \qquad (2.3)$$

Where V_{EB} is the applied voltage at the emitter-base junction. It is assumed that the electric field at the base-collector junction is large enough to saturate the electron velocity. Then the electron concentration at the base-collector junction is [33]

$$n(W_B) = \frac{J_n}{qv_s} \qquad (2.4)$$

By putting (2.2) in (2.1) and using boundary conditions from (2.3) and (2.4) collector current equation can be found:

$$J_C = J_{CO}\, e^{\left(\frac{qV_{BE}}{kT}\right)} = \frac{qe^{\left(\frac{qV_{BE}}{kT}\right)}}{\int_0^{W_B} \frac{N_B(x)}{n_{ieInGaAs}^2(x) D_{nSiGe(x)}} dx + \frac{N_B(W_B)}{n_{ieInGaAs}^2(W_B) v_{sA}}} \quad (2.5)$$

Where J_{CO} is the collector saturation current density in Indium Gallium Arsenide HBT. $N_B(x)$ is the base doping profile; x is the length along base. W_B is the base width and v_{SA} is the saturation velocity within the alloy, V_{BE} is base- emitter voltage, k is the Boltzman constant and T is the temperature in degrees kelvin. N_B (W_B) and $n_{ieInGaAs}$(W_B) is doping concentration and effective intrinsic carrier concentration at base-collector junction respectively.

The common emitter curren gain (β) can be found from equation (2.5)

$$\beta = \frac{J_{CO}}{J_{BO}} = \frac{\frac{q}{J_{BO}}}{\int_0^{W_B} \frac{N_B(x)}{n_{ieInGaAs}^2(x) D_{nInGaAs(x)}} dx + \frac{N_B(W_B)}{n_{ieInGaAs}^2(W_B) v_{sA}}} \quad (2.6)$$

Where J_{BO} is the base-saturation current density.

2.6.2. Early voltage

Early voltage is derived from its very basic form. J_{CO} is used in that form to get V_A. To incorporate various factors and for various base doping indium profiles this equation will be used in chapter 4.

For a particular V_{BE} from V_A can be found

$$V_A = J_C \left(\frac{\delta V_{BC}}{\delta J_{BC}}\right) V_{BE} = constant \quad (2.7)$$

Equation (2.7) can be modified as

$$V_A = J_C \left(\frac{\delta W_B}{\delta J_C} \frac{\delta V_{BC}}{\delta W_B}\right) V_{BE} = constant \quad (2.8)$$

By solving (2.8) and (2.5) Early voltage equation can be found:

$$V_A = \frac{qn_{ieInGaAs}^2(W_B)D_{nInGaAs}(W_B)}{C_{BC}} \times \left(\int_0^{W_B} \frac{N_B(x)}{n_{ieInGaAs}^2(x)D_{nInGaAs(x)}} dx + \frac{N_B(W_B)}{n_{ieInGaAs}^2(W_B)v_{sA}} \right) \tag{2.9}$$

2.6.3 Electric field

Electric field in the base can be written as which is used to make field dependent diffusivity function

$$E(x) = V_T \frac{d}{dx}\left[\ln(\mathrm{p(x)})\right] - \frac{1}{q}\frac{d \triangle E_g(x)}{dx} \tag{2.10}$$

Where

V_T Thermal voltage;

P Hole concentration in the base

$\triangle E_g(x)$ Apparent electrical band gap narrowing in the base, which can be expressed in terms of the effective

$$\triangle E_g(x) = KT\left[\ln\left(\frac{n_{ie}^2(x)}{n_i^2}\right)\right] \tag{2.11}$$

Substituting (2.11) into (2.10) we can get

$$E(x) = V_T \ \frac{d}{dx}\left[\ln\left(\frac{\mathrm{p\ (x)}}{\mathrm{n_{ie}^2(x)}}\right)\right] \tag{2.12}$$

(2.12) can be modified for InGaAs doped base as follows:

$$E(x) = \frac{KT}{q}\left(\frac{1}{p(x)}\frac{dp(x)}{dx} - \frac{1}{n_{ie}^2(x)}\frac{dn_{ie}^2(x)}{dx}\right) \tag{2.13}$$

2.7 CONCLUSION

In this chapter advantages of heterojunction bipolar transistors over bipolar transistors were discussed. Schematic diagram and cross section of *InGaAs* heterojunction bipolar transistors have been discussed. Some basic equations were written which will be derived in the next chapter.

CHAPTER 3

MATHEMATICAL ANALYSIS

3.1 INTRODUCTION

The Early effect is the variation in the width of the base due to a variation in the applied base-to-collector voltage. To obtain an analytical model for Early voltage (V_A) and common emitter current gain (β) for $In_{1-x}\,Ga_x\,As$ base heterojunction bipolar transistor (HBT) is of great importance for efficient device design. Within the framework of drift and diffusion approaches, an outstanding analytical model should consider the following important effects: (a) different In profiles with non-uniformly doped base (b) change in In dose and gradient (c) heavy doping or band gap narrowing effect (d) finite carrier velocity at the collector edge (e) dependence of mobility on electric field and doping concentration (f) high injection effects. In this chapter an analytical expression for V_A and β for uniform and exponential base doping $In_{1-x}\,Ga_x\,As$ *n+-p-n HBT* is derived considering all the above-mentioned effects. Band-gap narrowing (BGN) effect is considered to calculate effective intrinsic concentration ($n_{ieInGaAs}$) for both indium profile and base doping profile. Band-gap narrowing due to presence of indium is assumed to have a linear dependence on indium concentration. Effective intrinsic concentration of indium gallium arsenide is dependent on intrinsic carrier concentration of gallium arsenide. Electron saturation velocity in indium gallium arsenide alloy will differ from gallium arsenide material which is considered in diffusivity calculation. The electric field ($E_{lInGaAs}$) within the base is dependent on the effective intrinsic carrier concentration and hole concentration. To

incorporate filed dependency in diffusivity an empirical expression is used. And algebraic equation is used to express trapezoidal/triangular/box indium profile.V_A and β dependent on effective intrinsic carrier concentration ($n_{ieInGaAs}$), field dependent diffusion coefficient ($D_{nInGaAs}$) and electric field ($E_{lInGaAs}$). Generalized equations were derived for $n_{ieInGaAs}$, $D_{nInGaAs}$ and$E_{lInGaAs}$. Only a parameter is varied to indicate uniform and exponential types of base doping profiles. From the equations of $n_{ieInGaAs,}$ $D_{nInGaAs,}$ $E_{lInGaAs}$ an expression of V_A and β is derived later.

3.2 DERIVATION OF THE MODEL EQUATIONS

The mole fraction (y) distribution profiles of In (Indium) of an $n^+ - p - n$ In_{1-x} Ga_x As-base HBT is shown in Fig. 3.1 In mole fraction can be expressed as a function of distance along the base for a generalized trapezoidal profile

$$y(x) = m_{In}x + y_E \tag{3.1}$$

Where, x is the distance of a point in the base measured from the emitter-base (EB) junction of the HBT $m_{In} = \eta_{In}$ $/W_B$, W_B WB is the neutral base width, $\eta_{In} = y_C - y_E$and y_E are In fractions at the collector and emitter end of the base respectively. For $y_E = 0 \neq y_C$, $y_C = y_E$, $y_E = y_c \neq 0$ $r$epresents triangular,box and trapizoidal profile respectively, Total In content within the base termed as "In dose" is calculated as [40]

$$y_D = y_{av}W_B \tag{3.2}$$

$$y_{av} = (y_c + y_E)/2 \tag{3.3}$$

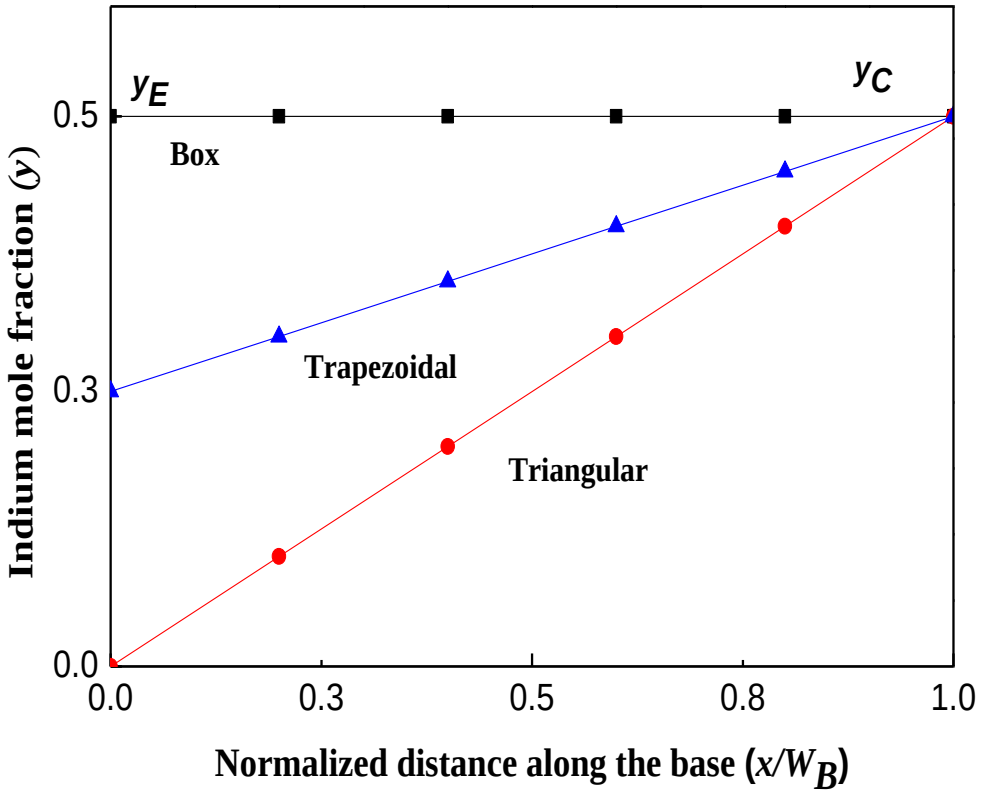

Figure 3.1: In (Indium) mole fraction distribution within the base of a $In_{1-x}\,Ga_x\,As$ HBT for various geometric profiles.

The schematic representation of an *n*+-*p*-*n* transistor is shown in Figure 2.2. The electron current density J_n and hole current density J_p with arbitrary base doping concentration *NB*(*x*) are given by the transport equations [41] [32]

$$-J_n(x) = qD_n(x)\frac{dn\,(x)}{dx} + q\mu_n(x)n(x)E(x) \qquad (3.4a)$$

$$J_p(x) = -qD_p(x)\frac{dp\,(x)}{dx} + q\mu_p(x)p(x)E(x) \qquad (3.4b)$$

where, $Dn(x)$ & $Dp(x)$ are the diffusion co-efficient (or diffusivity) for electron & hole, $\mu n(x)$ & $\mu p(x)$ are the electron & hole mobility, $n(x)$ & $p(x)$ are the electron & hole concentration respectively and $E(x)$ is the electric field at a point within the base. The direction of Jn in (2.4a) is defined such that it has a positive value. The total current density is the sum of the electron and hole current density.

$$J_c(x) = J_n(x) + J_p(x) \tag{3.5}$$

The electron diffusion length in GaAs ranging from 3.2 μ at low carrier concentration (6.9×10^{16} cm^{-3}) to 0.6 μ at high carrier concentration (3.76×10^{19} cm^{-3})[44] As the base width of a modern high-speed HBT is very thin (less than 100nm even 26nm base width is reported in [40]), the carrier recombination in the base region can safely be neglected. So,

$$J_p(x) = 0 \tag{3.6a}$$

$$J_c(x) \cong J_n(x) \tag{3.6b}$$

Therefore, the minority carrier current density J_n within the base becomes constant and is equal to collector current density J_c. In the present work, minority carrier concentration at thermal equilibrium has been neglected.

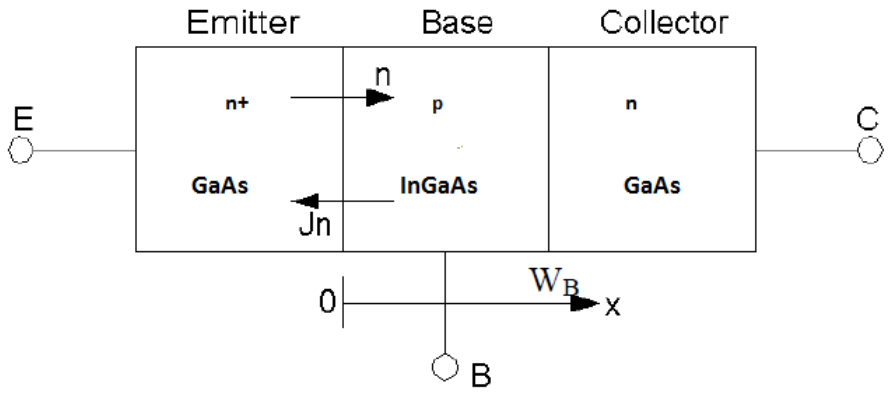

Figure 3.2: One-dimensional view of an *n-p-n* $In_{1-x}\,Ga_x\,As$- heterojunction bipolar transistor showing flow of injected minority carrier and current density.

The electric field neglecting recombination in the base and considering band gap narrowing effect is [40] [43]

$$E(x) = V_T \ \frac{d}{dx}\left[ln\left(\frac{p\,(x)}{n_{ie}^2(x)}\right)\right] \tag{3.7a}$$

where, V_T is the thermal voltage and is equal to *kT/q*, *k* is the Boltzmann constant, *T* is the temperature in degrees Kelvin, $n_{ie}(x)$ is the effective intrinsic carrier concentration in the base.

Equation (3.7a) can be written as follows [41]

$$E(x) = V_T\left(\frac{1}{p(x)}\frac{dp(x)}{dx} - \frac{1}{n_{ie}^2(x)}\frac{dn_{ie}^2(x)}{dx}\right) \tag{3.7b}$$

The first term in (3.7b) represents electric field due to concentration gradient and the second term in (3.7b) represents the quasi-field due to non-uniform band-gap narrowing. Carrier mobility and diffusivity are correlated as described by the Einstein's relation [45]

$$D_n(x) = V_T \mu_n(x) \tag{3.8}$$

The quasi-neutrality of charge within the base of a bipolar transistor is [45]

$$p(x) = n(x) + N_B\,(x) \tag{3.9}$$

For low injection, the quasi-neutral condition (3.9) becomes [58]

$$p_l(x) = n_l(x) + N_B(x) \approx N_B(x) \tag{3.10}$$

Base doping concentration for uniform and exponential base doping profiles is given by (3.11a) and (3.11b) respectively:

$$N_B(x) = N_B(0) \tag{3.11a}$$

$$N_B(x) = N_B(0)\, e^{-m_{exp}x} \tag{3.11b}$$

Where

$$m_{exp} = \frac{\ln(N_B(0)/\, N_B(W_B)\,)}{W_B} \tag{3.12}$$

$N_B(0)$ And $N_B(W_B)$ is the peak base doping concentration at the base-emitter and base-collector junction respectively.

Diffusivity equation can be written for impurity doping in GaAs base [32]

$$D_{nGaAs}(x) = D_n \tag{3.13a}$$

$$D_{nGaAs}(x) = D_n e^{m_{1\,exp}x} \tag{3.13b}$$

Equation (3.13a) and (3.13b) represents diffusion coefficient for uniform and exponential doping profile respectively,

Where

$D_n = D_{no}\left(\frac{N_B(0)}{N_r}\right)^{-\gamma_1}$, $D_{no} = 103.6\ \frac{cm^2}{s}$, $N_r = 10^{17} cm^{-3}$

$$m_{1\,exp} = m_{exp}\gamma_1 \text{ and } \gamma_1 = 0.43.$$

In the presence of *In*, the electron diffusivity is modified as [47]

$$D_{nInGaAs}(x) = b\, D_{nGaAs}(x) \tag{3.14a}$$

Where, b=1+3y_{av}.

The saturation velocity inside the *InGaAs* alloy also differs from that in GaAs and is [48]

$$V_{sA} = c\, v_s \tag{3.14b}$$

Where, c=0.342/ [0.342+y_{av} (1-y_{av})] and v_s=1.4×10^7 cm/s is the saturation velocity in GaAs.

The empirical expression for high field and doping dependent mobility in GaAs is [49]

$$\mu_{nGaAs}(|E|,x) = \frac{V_s}{a|E| + E_{cGaAs}(x)} \tag{3.15a}$$

Where, a=0.7743. $E_{cGaAs}(x)$ is the critical electric field and given by

$$E_{cGaAs}(x) = \frac{V_s}{\mu_{nGaAs}(x)} \tag{3.15b}$$

The effective intrinsic concentration in InGaAs is [47]

$$n^2_{ieInGaAs}(x) = \gamma(x) n^2_{ioGaAs} e^{\frac{\Delta E_{geff}(x)}{KT}} \tag{3.16a}$$

where, n_{ioGaAs}=1.79x10^6 cm^{-3} is intrinsic carrier concentration in undoped GaAs, *γ(x)* is the ratio of the effective density of states in InGaAs to the effective density of states in GaAs as given in [43]

$$\gamma(x) = \exp[-\sqrt{5y(x)}] \tag{3.16b}$$

Throughout the analysis $\gamma(x)$ considered varying in the base region but only to make close from V_A and β it is considered fixed [51]

$$y_r = \exp[-\sqrt{5y_{av}}] \tag{3.16c}$$

Δ*Egeff*(*x*) is the effective bandgap reduction in the InGaAs base that can be expressed as

$$\Delta E_{geff}(x) = \Delta E_{gHD}(x) + \Delta E_{gIn}(x) \tag{3.16d}$$

where $\Delta E_{gIn}(x)$ is the bandgap narrowing due to the presence of *In* which is assumed to have a linear dependence on In concentration, $\Delta E_{gHD}(x)$ is the bandgap narrowing

due to heavy doping effects [13]. An approximation of the Slotboom–de Graff bandgap narrowing model [52] is used for this term [53]

$$\Delta E_{gHD}(x) = q\, V_{gHD} \ln\left(\frac{N_B(x)}{N_r}\right) \tag{3.16e}$$

with, V_{gHD}=18 mV & the bandgap narrowing due to the presence of In is given by [54]

$$\Delta E_{gIn}(x) = q\, V_{gIn}\, y(x) \tag{3.16f}$$

with, V_{gIn} =750 mV. Combining (3.16a)-(3.16f), effective intrinsic concentration in InGaAs can be expressed as

$$n^2_{ieInGaAs}(x) = n^2_{ioGaAs} e^{\gamma_3 \gamma_e} \left(\frac{N_B(0)}{N_r}\right)^{\gamma_2} e^{(m_3 x - m_2 x^{\alpha})}.\gamma(x) \tag{3.16g}$$

Where, $\gamma_2 = {V_{gHD}}\big/{V_T} = 0.69, \gamma_3 = {V_{gGe}}\big/{V_T} = 28.84, m_3 = \gamma_3.m_{In}$

m_2 for uniform and exponential will be 0 and $m_{exp}.y_{2.}\alpha$ for uniform and exponential base doping profile will be 0 and 1 respectively.

3.2.1 Model of early voltage and current gain

Low injection conditions for a pn junction refers to the state where the numbers of carriers generated are small compared to the background doping density of the material.

The subscript $'l'$ stands for low injection value of the associated parameter hereafter.from (3.7b) & (3.16),electric field distribution throughout the base of a InGaAs HBT becomes[57]

$$E_{lInGaAs}(x) = V_T \left(\frac{1}{N_B(x)}\frac{dN_B(x)}{dx} - \frac{1}{n^2_{ieInGaAs}(x)}\frac{dn^2_{ieInGaAs}(x)}{dx}\right) \tag{3.17a}$$

Using 3.11(a,b),(3.16g) and (3.17a),electric field under low injection will be:

$$E_{lInGaAs}(x) = V_T \left(m_3 + 0.31\alpha m x^{(\alpha-1)} - \left(\frac{m_{In}\sqrt{5}}{2}\right)\frac{1}{\sqrt{m_{In}x+y_E}} \right) \quad (3.17b)$$

Value for m for uniform and exponential will be 0 and $m_{exp}.y_{2.}\alpha$ for uniform and exponential base doping profile will be 0 and 1 respectively.

For arbitrary doped base HBT with arbitrary Indium profile, the collector current density can be expressed as [54] [55]

$$J_C = J_{CO}\, e^{\left(\frac{qV_{BE}}{kT}\right)} = \frac{qe^{\left(\frac{qV_{BE}}{kT}\right)}}{\int_0^{W_B} \frac{N_B(x)}{n^2_{ieInGaAs}(x)D_{nSiGe(x)}}dx + \frac{N_B(W_B)}{n^2_{ieInGaAs}(W_B)v_{sA}}} \quad (3.18a)$$

The collector saturation current density in Indium gallium arsenide HBT is J_{CO} .V_{BE} is base emitter voltage.$N_B(W_B)$ and $n_{ieIn\,GaAS}\,(W_B\,)$ is doping concentration and effective intrinsic carrier concentration at base-collector junction respectively.

The common emitter current gain (β) can be found from equation (3.18a)

$$\beta = \frac{J_{CO}}{J_{BO}} = \frac{\frac{q}{J_{BO}}}{\int_0^{W_B} \frac{N_B(x)}{n^2_{ieInGaAs}(x)D_{nInGaAs(x)}}dx + \frac{N_B(W_B)}{n^2_{ieInGaAs}(W_B)v_{sA}}} \quad (3.18b)$$

Where, J_{BO} is the base saturation current density.

Early voltage is defined as

$$V_A = J_C \left(\frac{\delta W_B}{\delta J_C}\frac{\delta V_{BC}}{\delta W_B} \right) V_{BE} = constant \quad (3.19a)$$

Where V_{BC} is the base to collector voltage

The early voltage can be derived by using equation (3.18a) in (3.19a) and is given

$$V_A = \frac{qn^2_{ieInGaAs}(W_B)D_{nInGaAs}(W_B)}{C_{BC}} \times \left(\int_0^{W_B} \frac{N_B(x)}{n^2_{ieInGaAs}(x)D_{nInGaAs(x)}}dx + \frac{N_B(W_B)}{n^2_{ieInGaAs}(W_B)v_{sA}} \right)$$

(3.19b)

Where C_{BC} is the base-collector junction capacitance .

From equation (3.18b) and (3.19b),product of current gain-early voltage (βV_A) becomes

$$\beta V_A = \frac{q^2 n_{ieInGaAs}^2(W_B) D_{nInGaAs}(W_B)}{J_{BO} C_{BC}} \tag{3.19c}$$

Eq (3.14a), (3.15a) and (3.17b) is used to calculate $D_{nInGaAs}(x)$.By using the value of $D_{nInGaAs}$, $n_{ieInGaAs}^2$ and $E_{lInGaAs}(x)$.It can be found β and V_A from (3.18b) and (3.19b) respectively.

By considering ratio of effective density of states in InGaAs to that in silicon fixed throughout the base region[51] and then (3.16g) and (3.17b) minimizes to (3.20) and (3.21) respectively:

$$n_{ieInGaAs}^2(x) = n_{ieSiGe}^2 InGaAs(0).e^{(m_3 x - m_2 x^a)} \tag{3.20}$$

Where $n_{ieInGaAs}^2(0) = n_{ioGaAs}^2 e^{\gamma_3 y_e}(N_B(0)/N_r)^{y2}.y_r$

$$E_{lInGaAs}(x) = V_T\,(m_3 + .31\alpha m x^{\alpha-1}) \tag{3.21}$$

For exponential base doping profile,

$$V_A = (I_1 + \frac{N_B(W_B)}{n_{ieInGaAs.}^2 v_{sA}})(\frac{q n_{ieInGaAs}^2(W_B)}{c})(\frac{b v_s D_n e^{m1 W_B}}{V_s + a m_{032} D_n e^{m1 W_B}}) \tag{3.22}$$

Where

$$I_1 = \frac{N_B(0)\, a\, m_{032}}{n_{ieInGaAs}^2(0) b v_s\ m_{132}}(1 - e^{-m_{132} W_B}) + \frac{N_B(0)}{n_{ieInGaAs}^2(0) b D_n m_{0132}}(1 - e^{-m_{0132} W_B}) \tag{3.23}$$

And $m_{32} = m_3 - m_2$, $m_{032} = m + m_3 - m_2$, $m_{132} = m_1 + m_{32}$, $m_{0132} = m + m_1 + m_{32}$.

For exponential base doping profile can be found by the expression given below:

$$\beta = \frac{J_{CO}}{J_{BO}} = \frac{{}^{q}/_{J_{BO}}}{I_1 + \frac{N_B(W_B)}{n_{ieInGaAs}^2(W_B)v_{SA}}} \tag{3.24}$$

For uniform base doping profile,

$$V_A = \left(I_2 + \frac{N_B\,(0)}{n_{ieInGaAs.}^2 v_{sA}}\right)\left(\frac{qn_{ieInGaAs}^2(W_B)}{c}\right)\left(\frac{bv_sD_n}{am_3D_n + V_s}\right) \tag{3.25}$$

Where

$$I_2 = \frac{N_B\,(0)(am_3D_n + V_s)}{n_{ieInGaAs}^2(0)bv_sD_n\,m_3}(1 - e^{-m_3W_B}) \tag{3.26}$$

For uniform base doping profile can be found by the expression given below:

$$\beta = \frac{J_{CO}}{J_{BO}} = \frac{{}^{q}/_{J_{BO}}}{I_2 + \frac{N_B(W_B)}{n_{ieInGaAs}^2(W_B)v_{SA}}} \tag{3.27}$$

3.3 CONCLUSION

The equations which were written in chapter 2 have been derived in this chapter. These equations will be used in next chapter to plot various graphs using MATLAB and ORIGIN.

CHAPTER 4

RESULT AND DISCUSSION

4.1 INTRODUCTION

The mathematical equations related to the analytical modeling of Early voltage and common emitter current gain of $In_{1-x}Ga_xAs$ base heterojunction bipolar transistor (HBT) have been derived in the previous chapter. To get numerical data MATLAB program was used. To show the effects of various parameters on V_A and β the numerical data generated by the program are plotted by using ORIGIN. The variation of intrinsic concentration, diffusivity, electric field, Early voltage, current gain with respect to various parameters are shown in graphical form separately for uniform and exponential profiles and then again also shown in same graph to compare the variation of both profiles. A discussion is made later on both profiles of various factors that influence these parameters.

4.2 RESULT AND DISCUSSIONS

For exponential base doping profile base doping concentration was considered as NB (0) $=10^{19}$ cm^{-3} and N_B (W_B) $=10^{17}$ cm^{-3} and for uniform base doping profile is considered 10^{19} cm^{-3}, base width W_B=50nm is considered for whole analysis. The results that found by using the derivations in the previous chapter are analyzed and discussed below.

4.2.1 Distribution of minority carrier within the base ($n_{ieInGaAs}$)

Effective intrinsic carrier concentration ($n_{ieInGaAs}$) distribution throughout the base region for uniform and exponential base doping is shown from Figure 4.1a through Figure 4.1c for fixed value of y_C and y_E (y_E is kept 0.01 and y_C is considered for two values 0.01 and 0.5). For same value of y_C and y_E, it is observed from Figure 4.1a that the value of $n_{ieInGaAs}$ has no changes for uniform base doping profile in the base region but it increases exponentially towards base-collector junction when y_E and y_C are not same (for y_E=0.01 and y_C=0.5).Again from Figure 4.1b it is observed that for exponential base doping profile when y_C and y_E are same $n_{ieInGaAs}$ gradually decreases towards base-collector junction but when y_C and y_E are not same (for y_C=0.5 and y_E=0.01) $n_{ieInGaAs}$ increases exponentially. Relative variation for both profiles can be observed from Figure 4.1c.For exponential base doping for small values of y_C (y_C=.01) $n_{ieInGaAs}$ is maximum at base-emitter junction and then decreases gradually toward base-collector junction but for large values of y_C (y_C=0.5) $n_{ieInGaAs}$ is minimum at base-emitter junction and then exponentially increases towards base-collector junction. For uniform base doping for same value of y_C and y_E, $n_{ieInGaAs}$ remains constant but for large values of y_C (for y_C=0. 5) $n_{ieInGaAs}$ gradually increases. This is due to BGN effect. Increasing y_C decreases band gap which in turns increases probability of carrier concentration in conduction band. BGN effects occurs for heavy doping and due to indium content .Heavy doping effect was discussed at Slotboom-de Graaf model [52] and BGN due to In(indium) content is discussed by Tyagi, S.D [56]. $n_{ieInGaAs}$ for HBT with y_C=0.5 is eleven times than normal BJT.

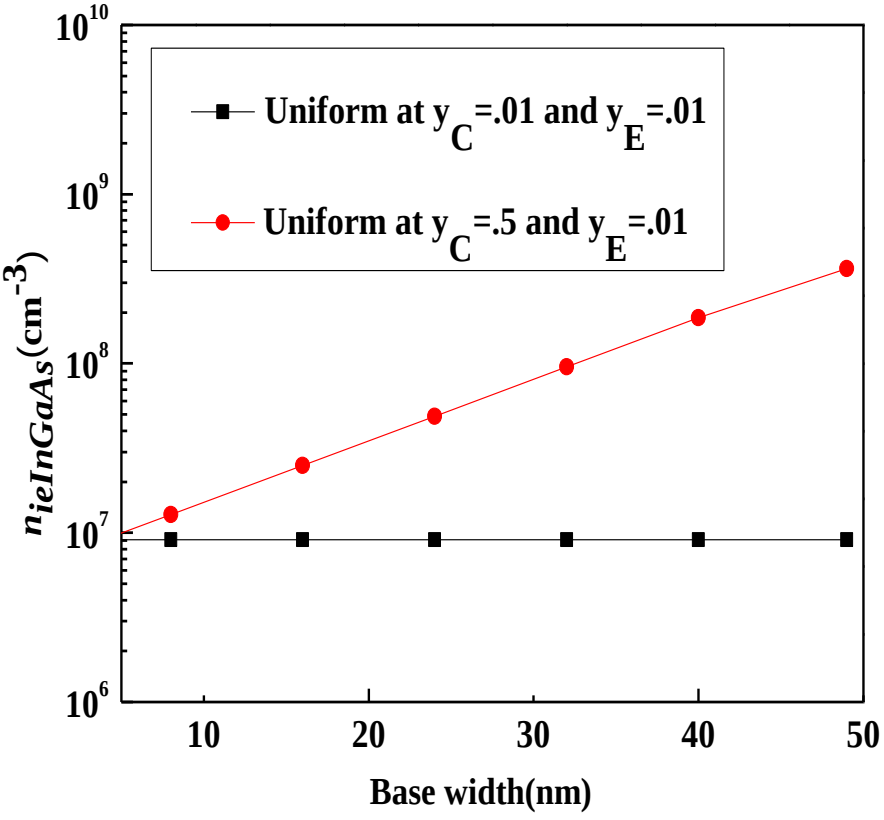

Figure 4.1a: Effective intrinsic carrier concentration $(n_{ieInGaAs})$ throughout the base region for uniform base doping profile for two value of y_c(0.01 and 0.5) and single value of y_E(0.01).

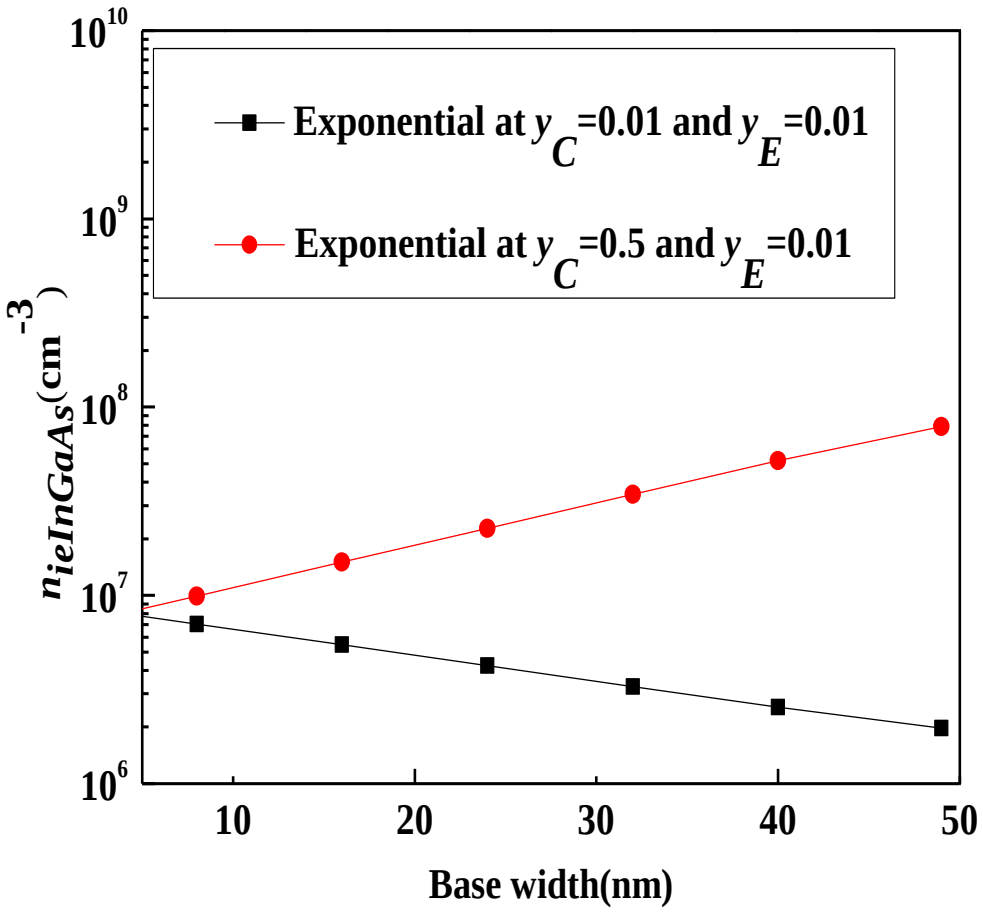

Figure 4.1b: Effective intrinsic carrier concentration ($n_{ieInGaAs}$) **throughout** the base region for exponential base doping profile for two value of y_c(0.01 and 0.5) and single value of y_E(0.01)

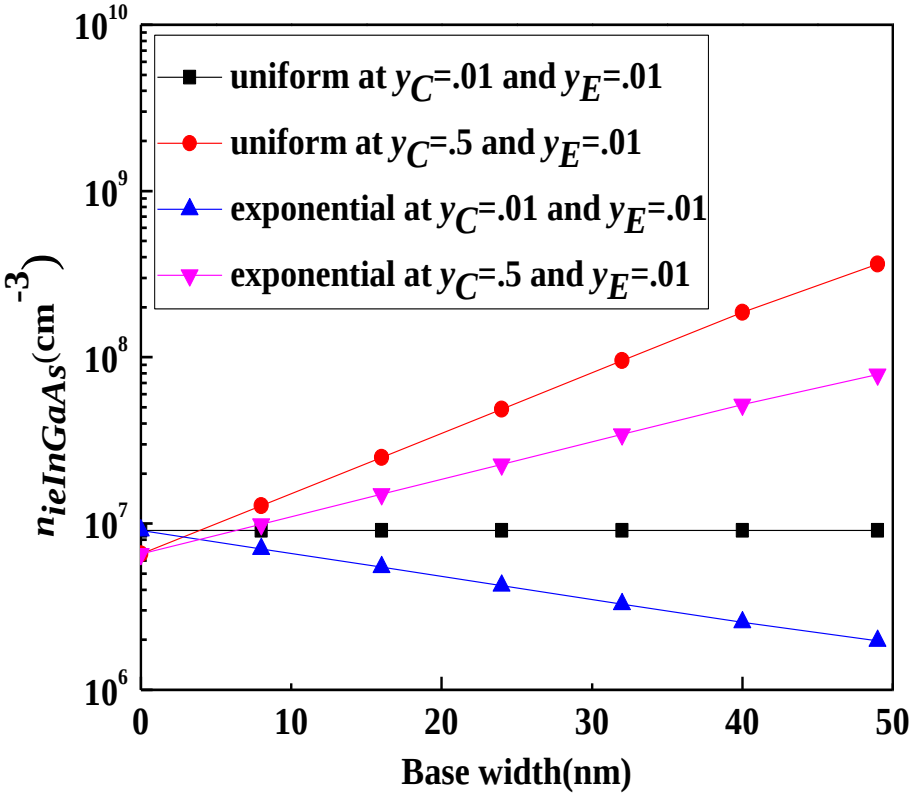

Figure 4.1c: Effective intrinsic carrier concentration $(n_{ieInGaAs})$ **throughout** the base region for uniform and exponential base doping profiles for two value of y_c(0.01 and 0.5) and single value of y_E(0.01).

Effective intrinsic carrier concentration $(n_{ieInGaAs})$ at base-emitter and base-collector junction for uniform and exponential base doping profiles are shown from Figure 4.2a to Figure 4.2c while varying y_C (.01~ 0.5) and fixed y_E (0.01). In the figure x=0 denotes base-emitter junction and x=W_B denotes base-collector junction. In Figure 4.2a it can be found that for uniform base doping $n_{ieInGaAs}$ remains constant at base-emitter junction while y_C increases but at base-collector junction when y_C increases $n_{ieInGaAs}$ increases exponentially. When y_C is low (0.01) the value of $n_{ieInGaAs}$ at both junction is same. In figure 4.2b it can be observed that for uniform base doping $n_{ieInGaAs}$ decreases a little bit(almost constant) at base-emitter junction while y_C increases but at base-collector

junction when y_C increases $n_{ieInGaAs}$ increases exponentially. In figure 4.2c a relative comparison is shown for both, uniform and exponential base doping profiles. From figure 4.2c it can be observed $n_{ieInGaAs}$ at base-collector junction for uniform is much greater than exponential base doping profile. Although BGN for uniform and exponential is same at base-collector junction for each yc, $n_{ieInGaAs}$ is greater for uniform base doping profile than exponential base-doping profile due to only difference in base doping profile. Base doping and BGN both are same at base-emitter junction for both profiles so $n_{ieInGaAs}$ is always same at this junction.

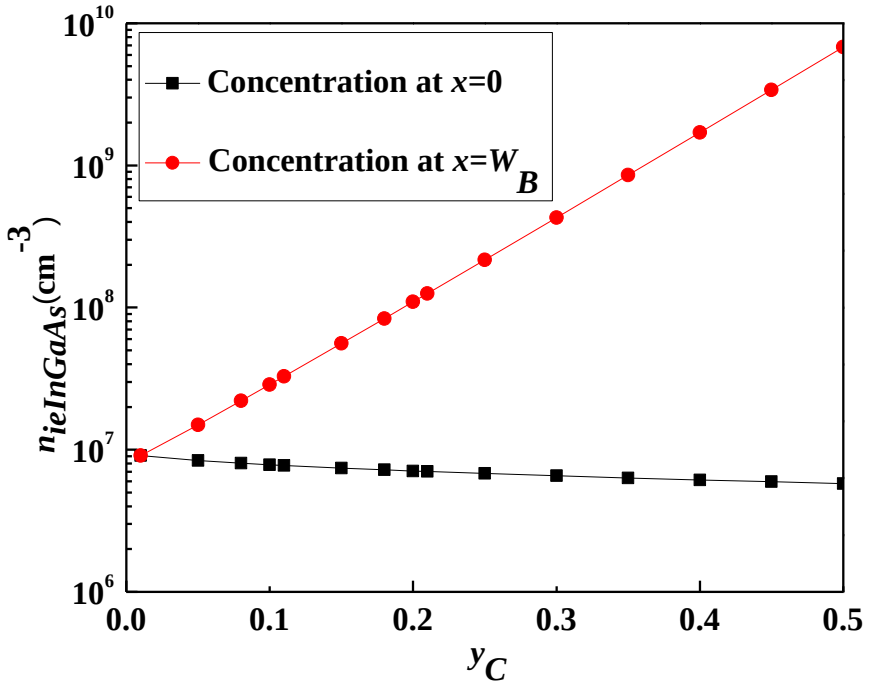

Figure 4.2a: Intrinsic carrier concentration at base-emitter junction*(x=0)* and base-collector junction *(x=W_B)* for varying y_c at uniform base doping profile.red line shows at base collector junction and black line shows $n_{ieInGaAs}$ at base emitter junction .In both case $y_E = .01$

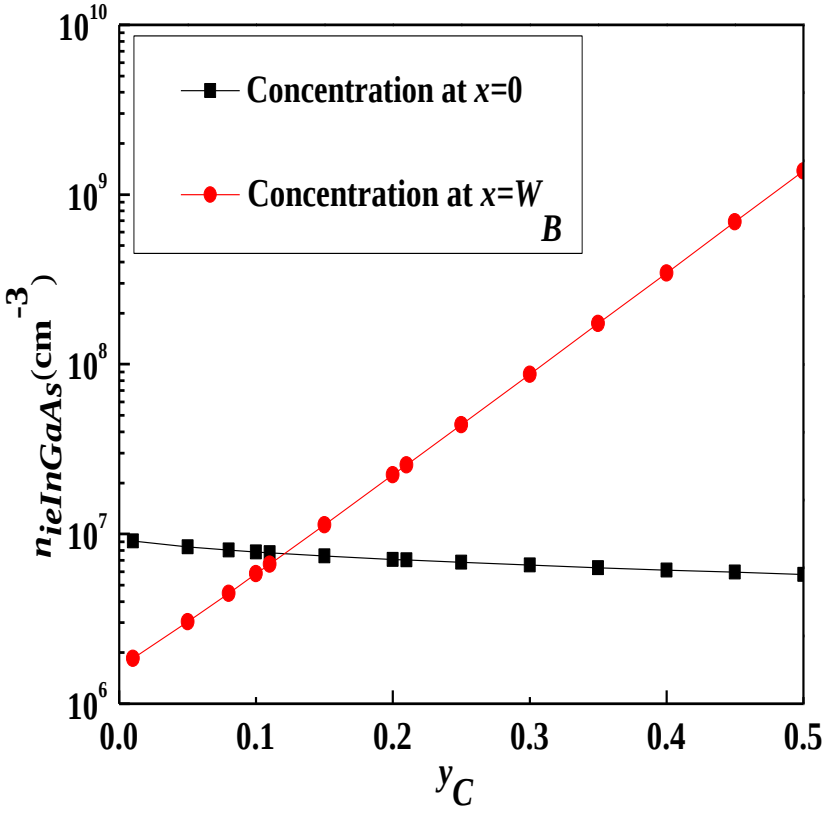

Figure 4.2b Intrinsic carrier concentration at base-emitter junction(x=0) and base-collector junction (x=W_B) for varying y_c at exponential base doping profile.red line shows at base collector junction and black line shows $n_{ieInGaAs}$ at base emitter junction .In both case $y_E = .01$

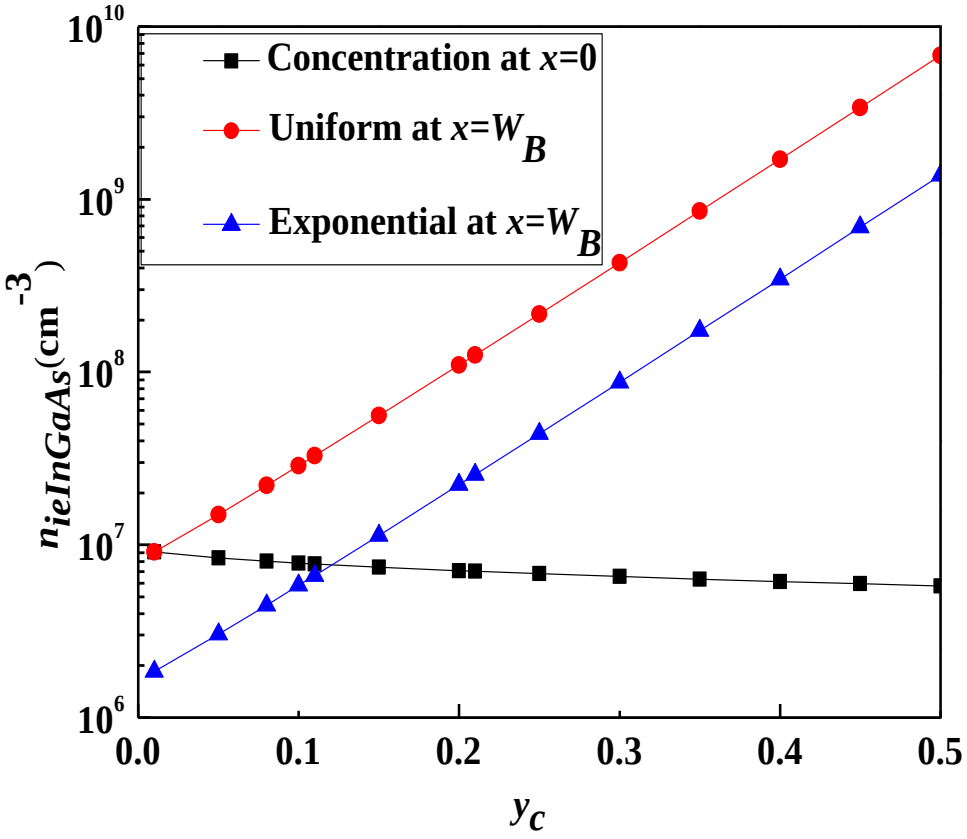

Figure 4.2c Intrinsic carrier concentration at base-emitter junction*(x=0)* and base-collector junction *(x=W_B)* for varying y_c at uniform and exponential base doping profile.Red line shows at base collector junction for uniform profile,.blue line shows at base collector junction for exponential profile and black line shows $n_{ieInGaAs}$ at base emitter junction for both .In both case $y_E = .01$

4.2.2 Electric field profile

Electric field at base-emitter and base-collector junction for uniform and exponential base profiles is shown from Figure 4.3 to Figure 4.3c.). In the figure x=0 denotes base-emitter junction and x=W_B denotes base-collector junction. It is known that increased indium enhance BGN ($\Delta Egeff$) which increases effective intrinsic carrier concentration ($n_{ieInGaAs}$) exponentially (Figure 4.2c). In Figure 4.3a electric field at base-emitter and base-collector junction for varying y_C and fixed y_E is shown. It shows that at both junction when y_C increases, electric field increases. As electric field is proportional ($\frac{dn_{ieInGaAS}(x)}{dx}$)o and when y_C increases the value of ($\frac{dn_{ieInGaAS}(x)}{dx}$) is much higher for base-collector junction than base-emitter junction ad it causes electric field to be higher at base-collector junction than base-emitter junction. So from Fig. 4.3a it can be observed that electric field at base-collector junction is higher than base-emitter junction. Fig 4.3b shows electric field for exponential base doping profiles which looks almost same as uniform base doping profile.

A comparison for uniform and exponential base-doping profiles can be observed form Figure 4.3c. At base-collector end electric field is lower for uniform than exponential base doping profiles because doping concentration at collector end for uniform doped base is greater than exponential base doping profiles but it has no variation throughout the base and as $n_{ieInGaAs}$ is much more higher for uniform than exponential doped base, so electric field is lower for uniform doped base at collector end as $n_{ieInGaAs}$ have reverse impact on electric field. On the other hand at base-emitter junction $n_{ieInGaAs}$ is same for both profiles but variation of base-doping is much more for exponential than uniform doped base so electric field is much higher for exponentially doped base than uniform base doping profiles at base-emitter junction. Built in electric difference between base-collector junction and base-emitter junction $(El_{InGaAs}(W_B) - El_{InGaAs}(0))$ has impact on electric speed, while passing through base-region if the value is higher electron will take smaller time.

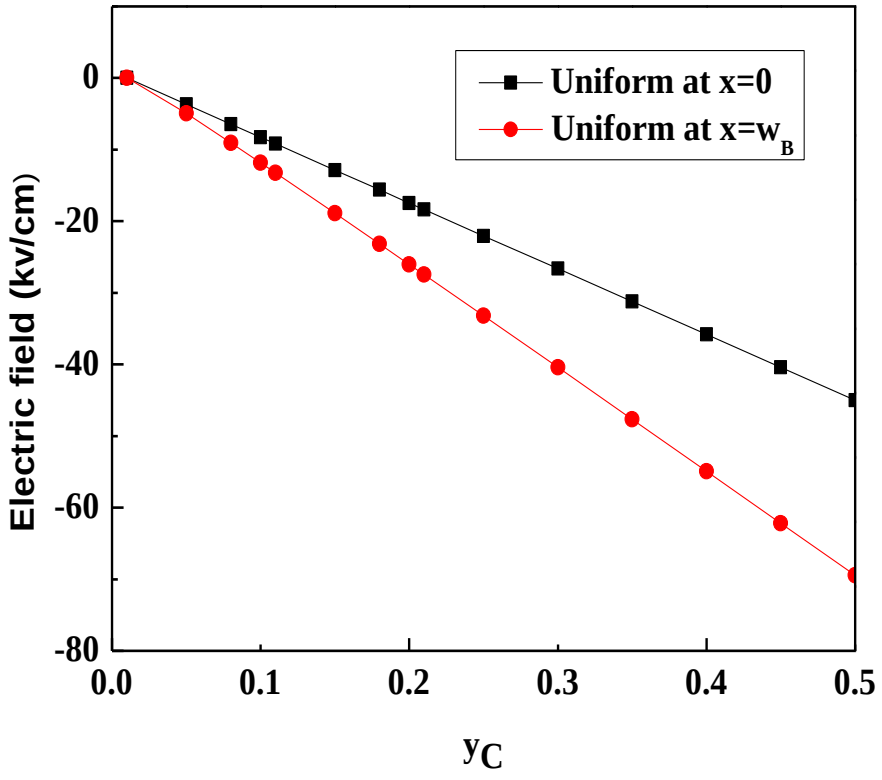

Figure 4.3a: Electric field at base-collector junction $E_{lInGaAs}(W_B)$ (Red line) and base-emitter junction $E_{lInGaAs}(0)$ (black line)for y_E=.01 and varying y_C (0.01 ~ 0.5) for uniform doping profile

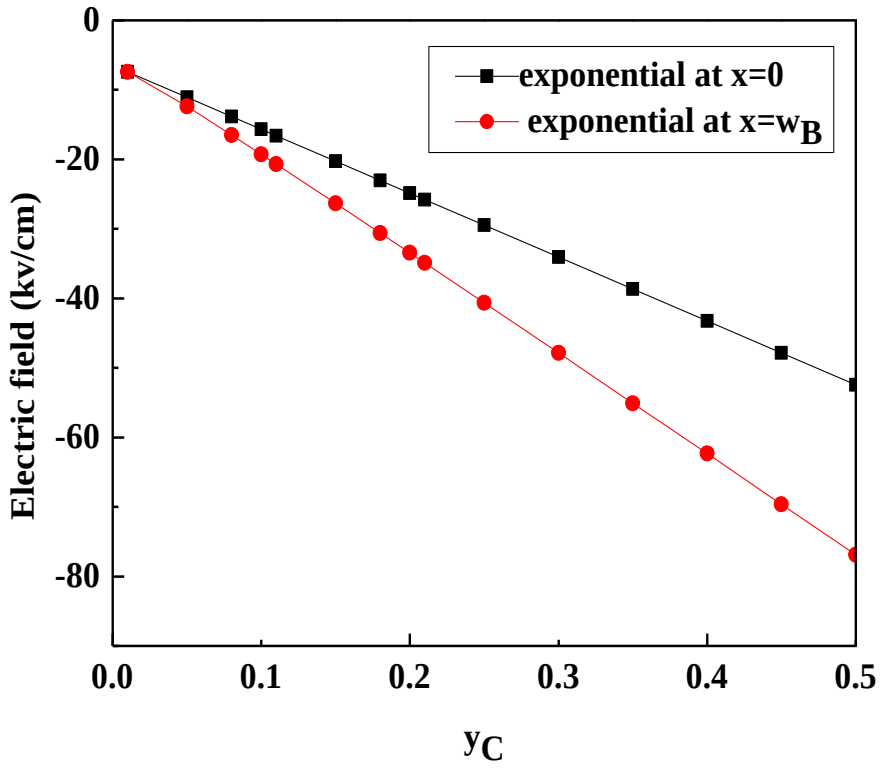

Figure 4.3b: Electric field at base-collector junction $E_{lInGaAs}$ (W_B) (Red line) and base-emitter junction $E_{lInGaAs}$ (0) (black line) for y_E=.01 and varying y_C (.01 ~ .5) for exponential doping profile

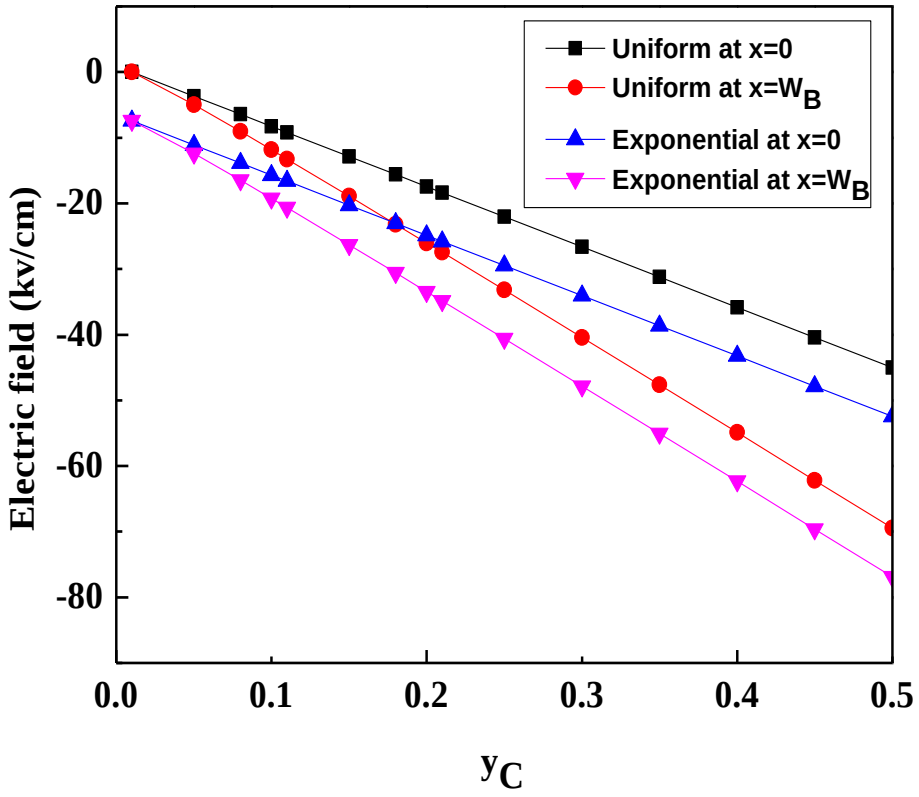

Figure 4.3c: Electric field at base-collector junction $E_{lInGaAs}(W_B)$ (Red line and pink line) and base-emitter junction $E_{lInGaAs}(0)$ (black line and blue line) for y_E=.01 and varying y_C(.01 ~ .5) for uniform and exponential profiles.

4.2.3 Diffusivity profile

Diffusivity with considering v_S effect for uniform and exponential base doping profiles are shown from Figure 4.4a to Figure 4.4c. Here y_E is fixed at 0.01 and y_E is fixed at 0.05 and N_B (0) is varied (from 10^{15} to 10^{20}). With considering v_S while N_B (0) increases diffusivity decreases for uniform doped base in Figure 4.4a. In Figure 4.4b for exponential base doping profile diffusivity decreases while N_B (0) increases.

Comparison for both profiles is shown in Figure 4.4c. From Figure. 4.4c it can be observed that for exponential base doping profile variation of diffusivity with $N_B(0)$ is less than uniform doped base profile. As diffusivity and mobility are related among them by a constant multiplying factor so diffusivity signifies mobility of electron.

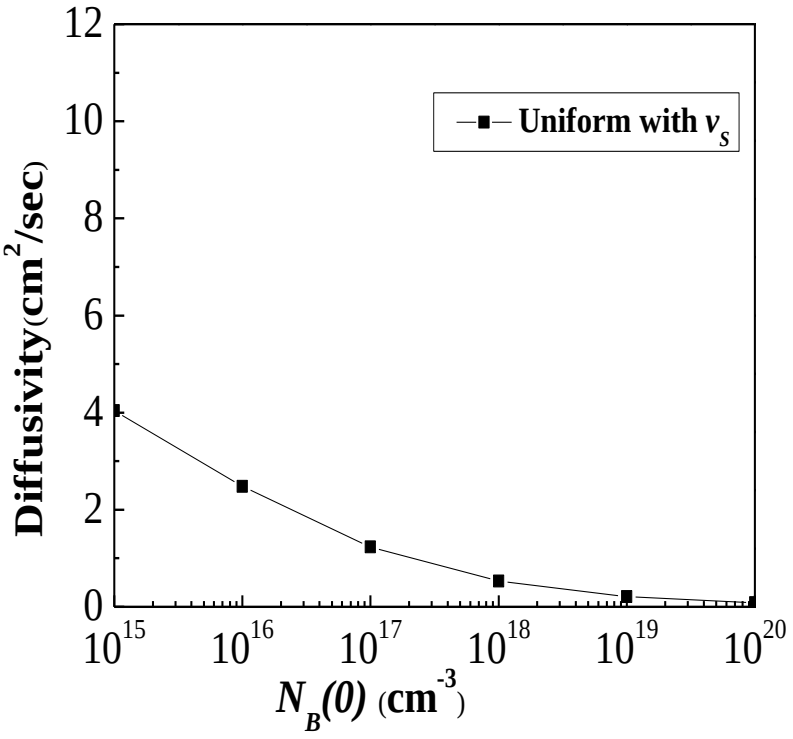

Figure 4.4a: Diffusion coefficient at base-collector junction $Dn_{InGaAs}(W_B)$ considering velocity saturation for y_E=.01,y_C=.5 and varying base doping $N_B(0)$ for uniform base doping profile.

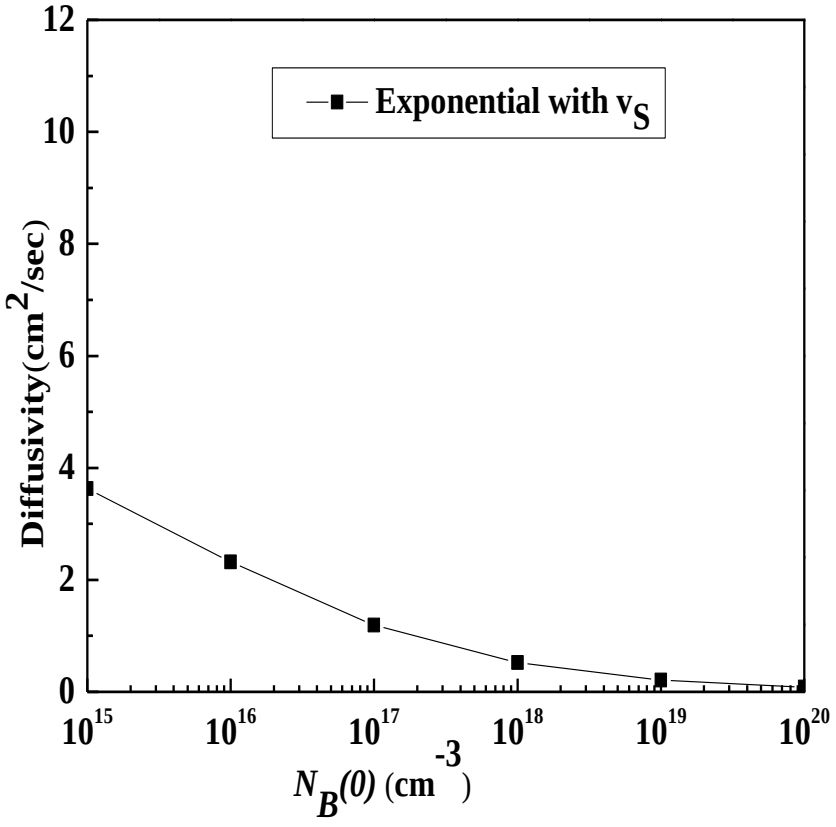

Figure 4.4b: Diffusion coefficient at base-collector junction $D_{nInGaAs}(W_B)$ considering velocity saturation for y_E=0.01,y_C=0.5 and varying base doping $N_B(0)$ for exponential base doping profile.

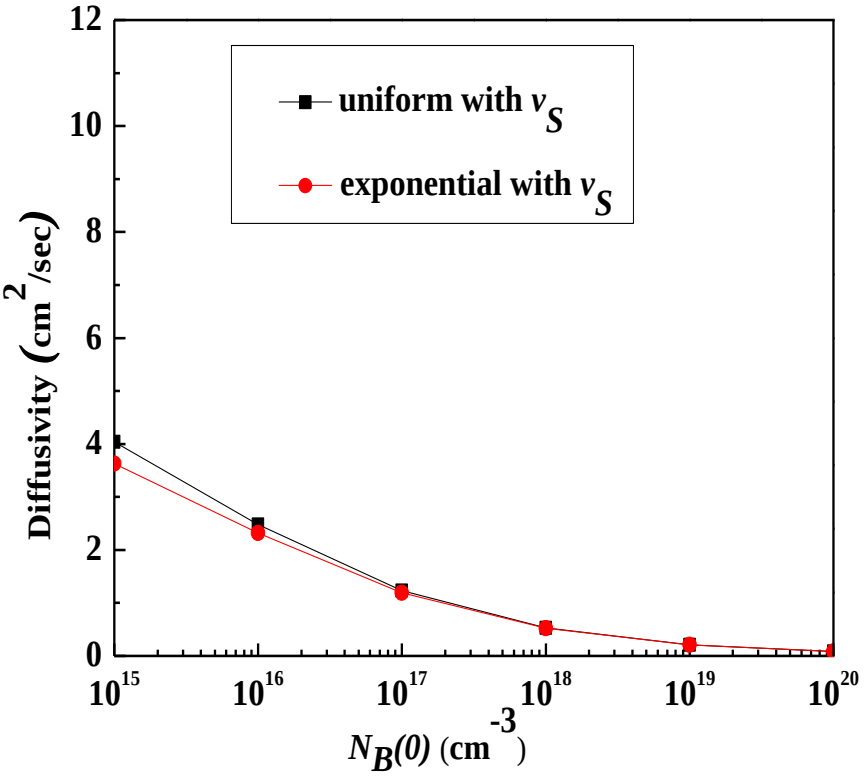

Figure 4.4c: Diffusion coefficient at base-collector junction $D_{nInGaAs}$ (W_B) considering velocity saturation for y_E =0.01, y_C =0.5 and varying base doping $N_B(0)$ for both uniform and exponential base doping profile.

4.2.3 Early voltage profile

Early voltage for uniform and exponential base doping profiles are shown from Fig. 1.5a to 4.5c where y_E is fixed at 0.01 and y_C is varied from 0.01 to 0.05.Early voltage increases exponentially with y_C. Base width, W_B is 500Å, peak doping at base-emitter junction is 10^{19} cm^{-3} and minimum doping at base-collector junction is 10^{17} cm^{-3} for exponential base doping profiles,10^{19} cm^{-3} is considered for uniform based doping profile. Figure 4.5a shows Early voltage for uniform base doping profile which increases exponentially with y_C. Figure 4.5b shows Early voltage for exponential base doping

profile. In Fig. 4.5c a comparison for both profiles is shown. From equation (3.19b) it can be observed that if effective intrinsic carrier concentration at the base-collector junction, $n_{ieInGaAs}(W_B)$ increases Early voltage V_A also increases. $n_{ieInGaAs}(W_B)$ is greater for uniform doped base than exponential base doping profile (Figure 4.2c) so V_A is greater for uniform doped base than exponential base doping profile

Early vltage for varying y_E with fixed y_C at 0.05 is shown in Figure 4.6. Here it is observed that by increasing y_E, V_A reduces exponentially for uniform and exponential base doping profiles. While y_E is increased, this results has no significant variation in $n_{ieInGaAs}(W_B)$ but it increases $n_{ieInGaAs}$ throughout the base region. If $n_{ieInGaAs}(W_B)$ is fixed but $n_{ieInGaAs}$ increases in the base region while increasing y_E, it reduces V_A (3.19b).

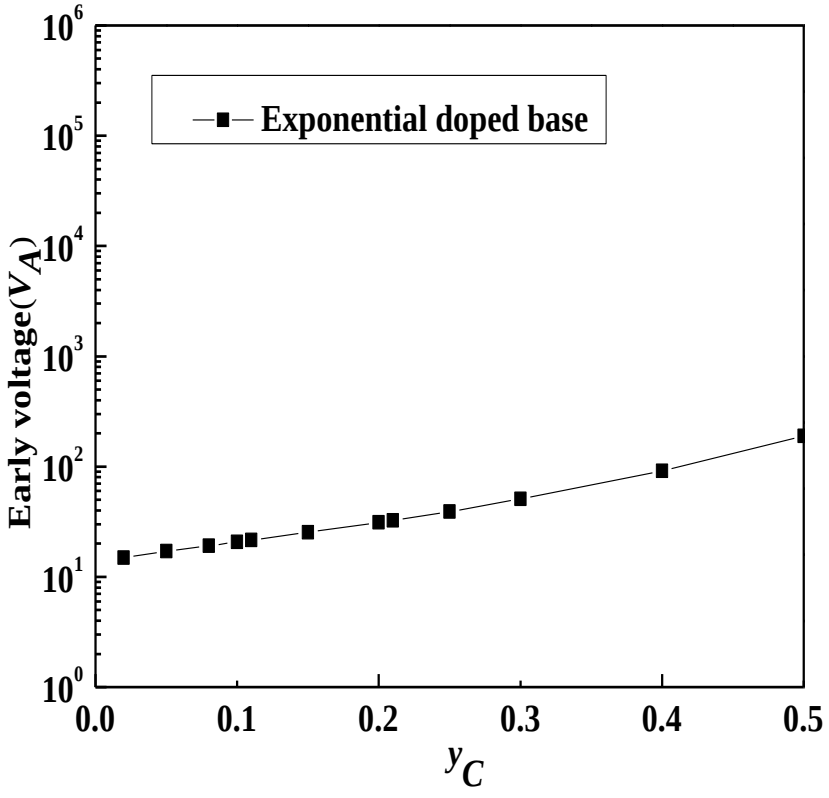

Figure 4.5a: Early voltage for y_E=.01 and varying y_C for uniform base doping profile. Base width W_B is 500Å, base doping is 10^{19} cm^{-3}

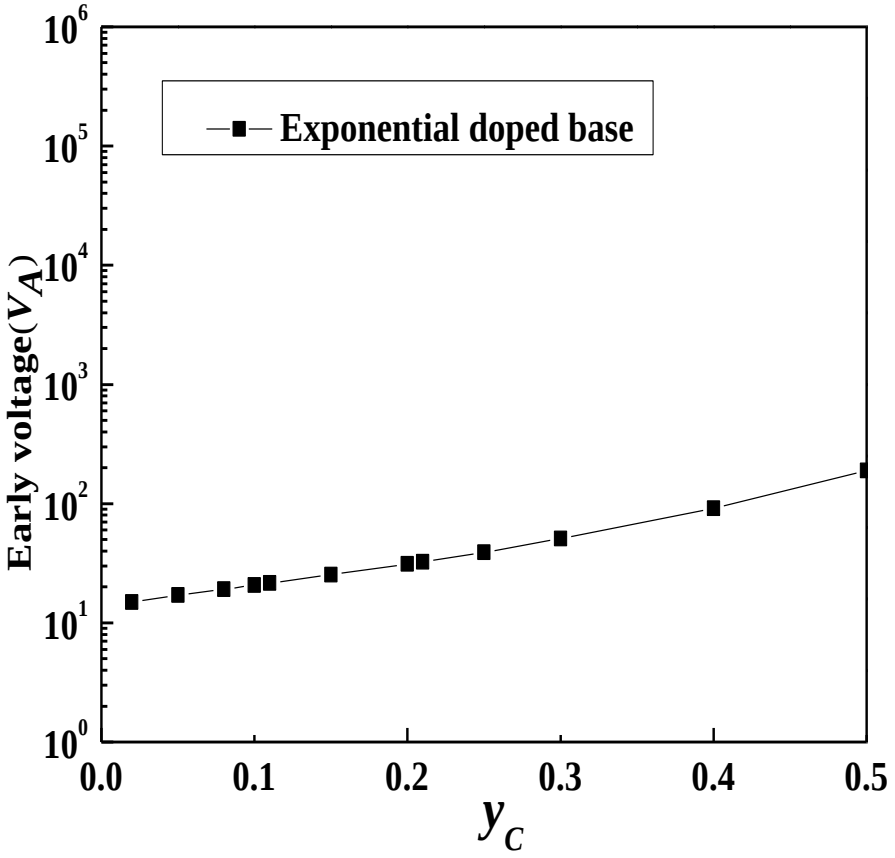

Figure 4.5b: Early voltage for y_E=.01 and varying y_C for exponential base doping profile. Base width W_B is 500Å, peak doping at base-emitter junction is 10^{19} cm-3 and minimum doping at base-collector junction is 10^{17} cm^{-3}.

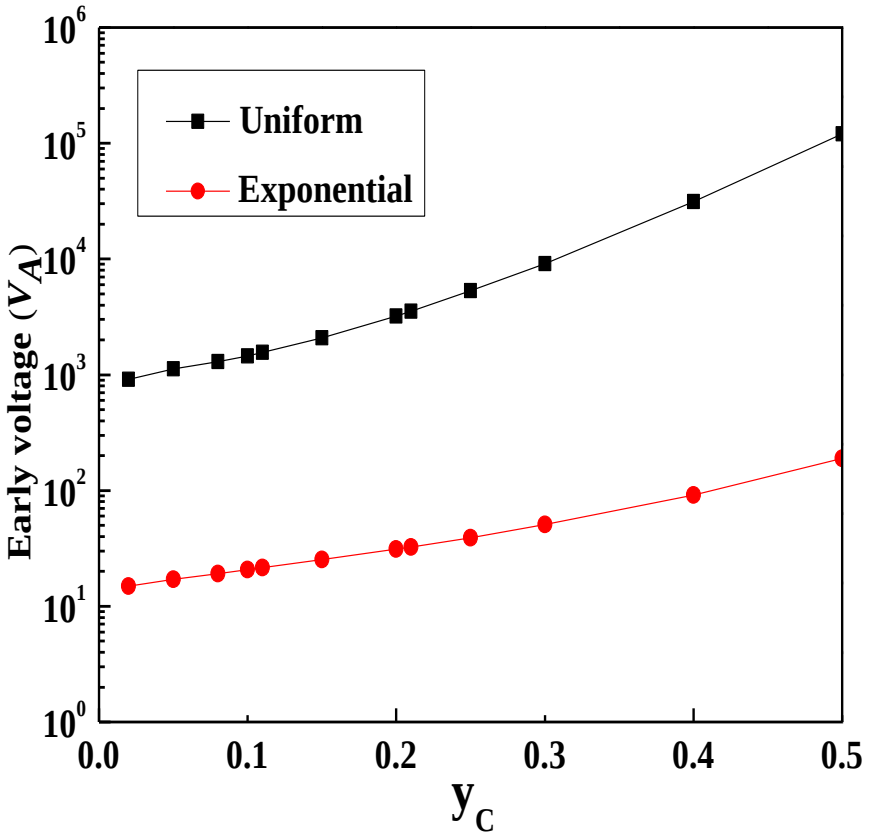

Figure 4.5c: Early voltages for y_E=.01 and varying y_C for uniform and exponential base doping profiles. Base width W_B is 500Å, peak doping at base-emitter junction is 10^{19} cm^{-3} and minimum doping at base-collector junction is 10^{17} cm^{-3} for exponential base profile and base doping is considered 10^{19} cm^{-3} for uniform base profile.

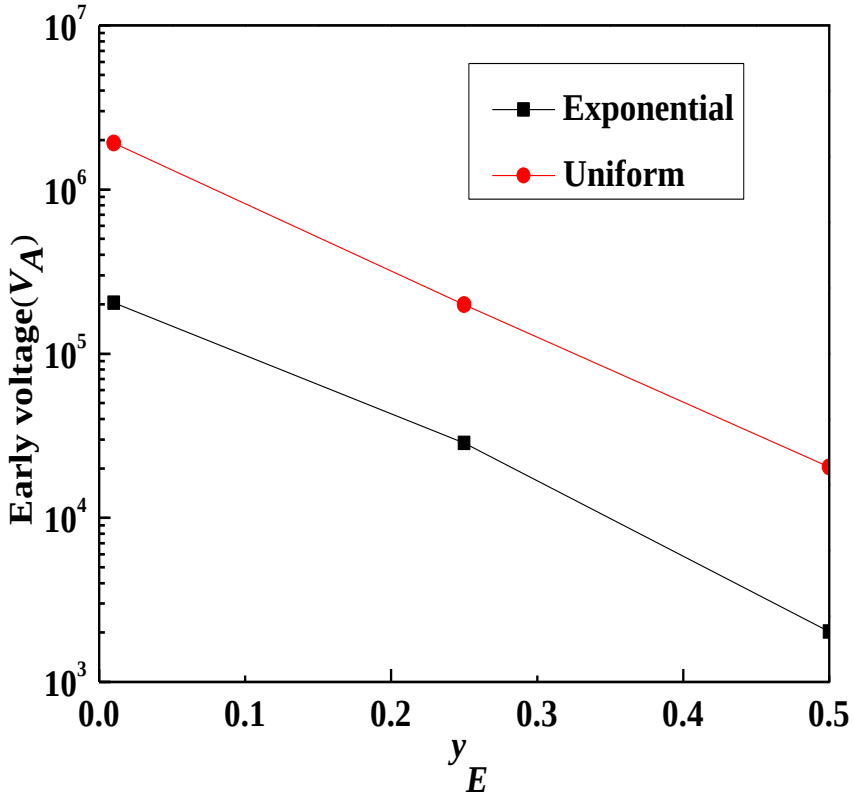

Figure 4.6: Early voltage for y_C=.5 and varying y_E for exponential and uniform base doping profiles. Base width, W_B is 500Å, peak doping at base-emitter junction is 10^{19} cm^{-3} and minimum doping at base-collector junction is 10^{17} cm^{-3}.

Concentration dependency of early voltage V_A for uniform and exponential base doping profiles is shown in Fig. 4.7a. It is observed that V_A is proportional to doping concentration. Doping concentration at base-collector junction for uniform doping N_B (W_B) =N_B (0) and for exponential doped N_B (W_B) =N_B (0)/100. It can be observed that Early voltage for uniform base doping profile is higher than exponential base doping profile. Depletion region created in the base is reduced by the overall increase of base doping concentration for a certain base doping concentration and reverse biased collector base voltage and thus Early effect is also reduced. The process which reduces

Early effect can increase Early voltage. So for increasing doping concentration Early voltage is increased.

Variation of V_A with exponential co-efficient m_{exp} for exponential base doping profile is shown in Figure 4.7b. Variation of m_{exp} is done by varying N_B (W). it is found from Fig. (3.12) that when $N_B(W_B)$ decreases, m_{exp} increases and V_A decreases.

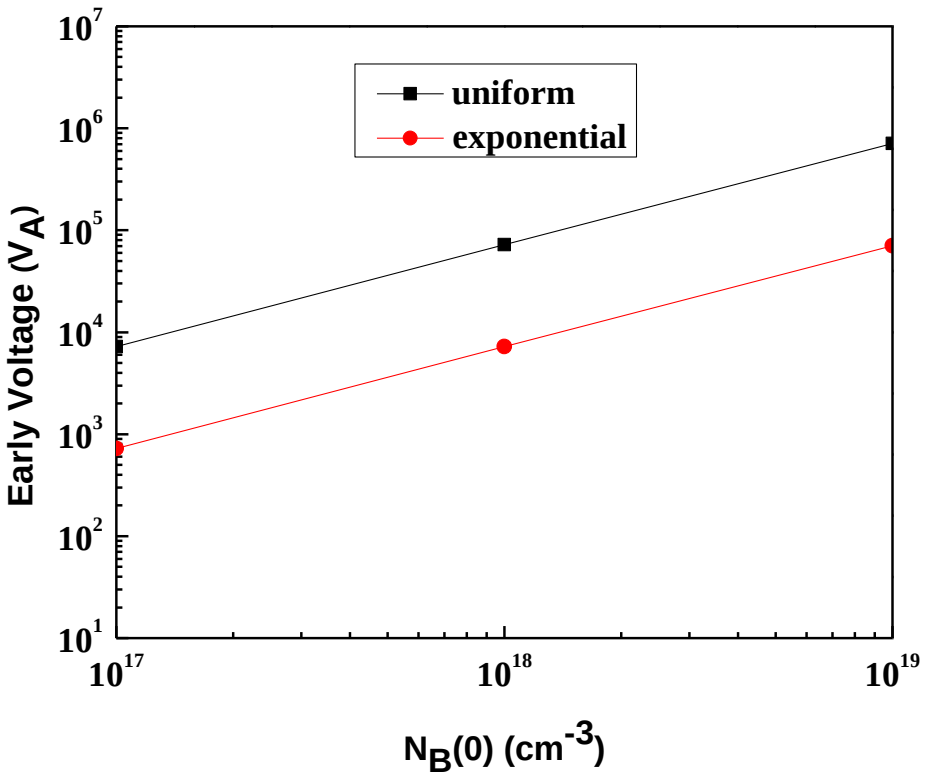

Figure 4.7a: Early voltage *(V_A)* for triangular indium profile with y_C=0.5 and y_E=0.01 with varying base doping. Doping concentration at base-collector junction for uniform doping $N_B\ (W_B) = N_B\ (0)$ and for exponential doped $N_B\ (W_B) = N_B\ (0)/100$

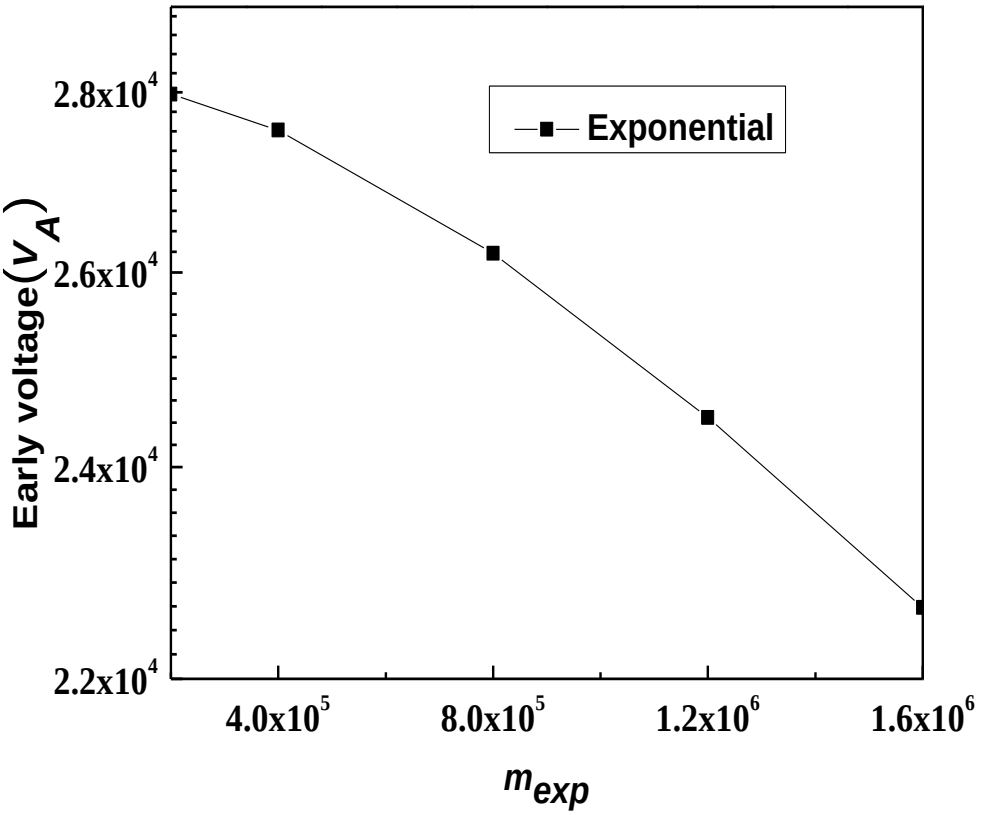

Figure 4.7b: Early voltage *(V_A)* for exponential doping profile with the variation of m_{exp}.

4.2.5 Collector saturation current density (J_{CO}) and common emitter current gain (β)

Dependence of collector saturation current density for uniform and exponential base doping profiles with varying y_C and fixed y_E at 0.01 is shown from Figure 4.8a to 4.8c. It can be observed in Fig. 4.8a that for uniform base doping profile J_{CO} decreases with the increase of y_C after slightly increasing with y_C. In Fig. 4.8b when y_C increases J_{CO} with v_S decreases for exponential base doping profile because electron velocity reaches its saturation value before reaching base-collector junction so if v_S is considered than electron velocity cannot overcome v_S and thus J_{CO} decreases. A comparison for both

profiles is given in Fig. 4.8c. It can be seen in Figure 4.8c is that J_{CO} is lower for exponential base doping than uniform doped base profile.

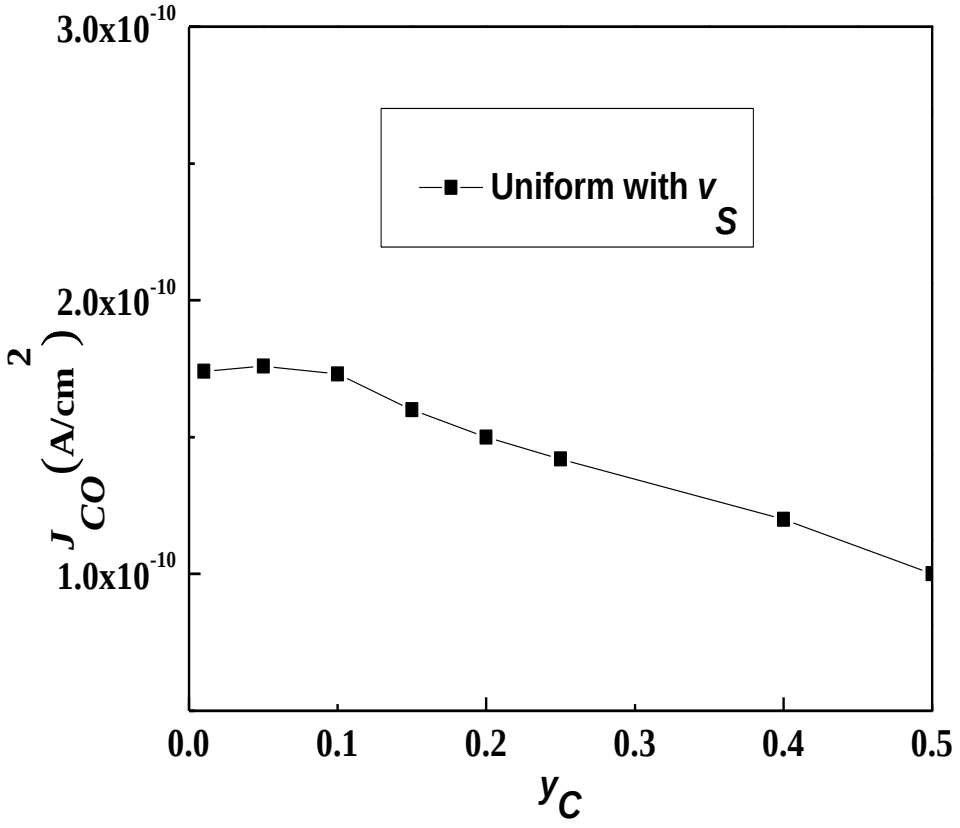

Figure 4.8a: Collector saturation current density *(J_{CO})* for fixed y_E (0.01) and varying y_C for uniform base doping profile.

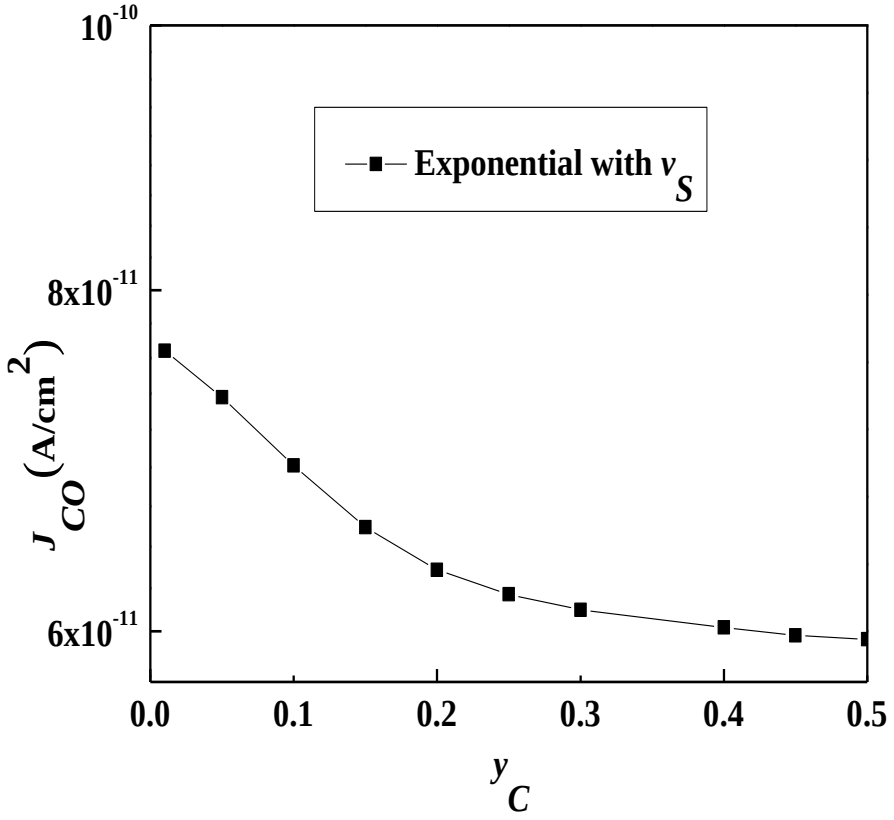

Figure 4.8b: Collector saturation current density *(J_{CO})* for fixed y_E(0.01) and varying y_C for uniform base doping profile.

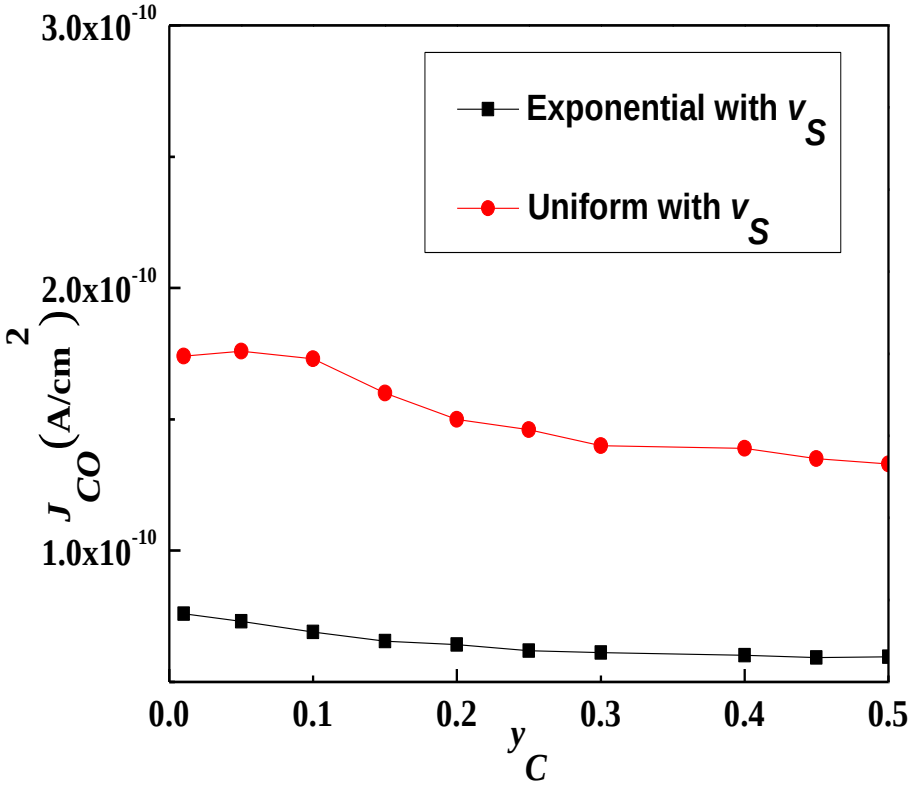

Figure 4.8c: Collector saturation current density (J_{CO}) for fixed y_E(0.01) and varying y_C for uniform and exponential base doping profile.

In Figure 4.9 common emitter current gain (β) for varying y_C and fixed y_E at 0. 2 is shown. it can be observed that for uniform doped base profile β increases while y_C increases but after certain value of y_C it starts reducing. Electron enters through emitter for an n-p-n transistor and due to electron hole recombination major parts of electrons pass towards collector with negligible loss in the base region. When y_C is small (~0.01) and y_E(~0.2), electron concentration is maximum near base-emitter junction and gradually decreases towards base-collector junction. While y_C increases in the base-collector junction which causes J_{CO} and β to be increased. After y_C (~0.2), electron concentration in collector-base junction is more than base-emitter junction which causes diffusion effect in the reverse direction to the normal electron flow from emitter to

collector. Moreover diffusivity also reduces by increasing y_C. These two effects decrease J_{CO} as well as β . But it can be observed that β starts decreases while y_C increases for exponential doped base.

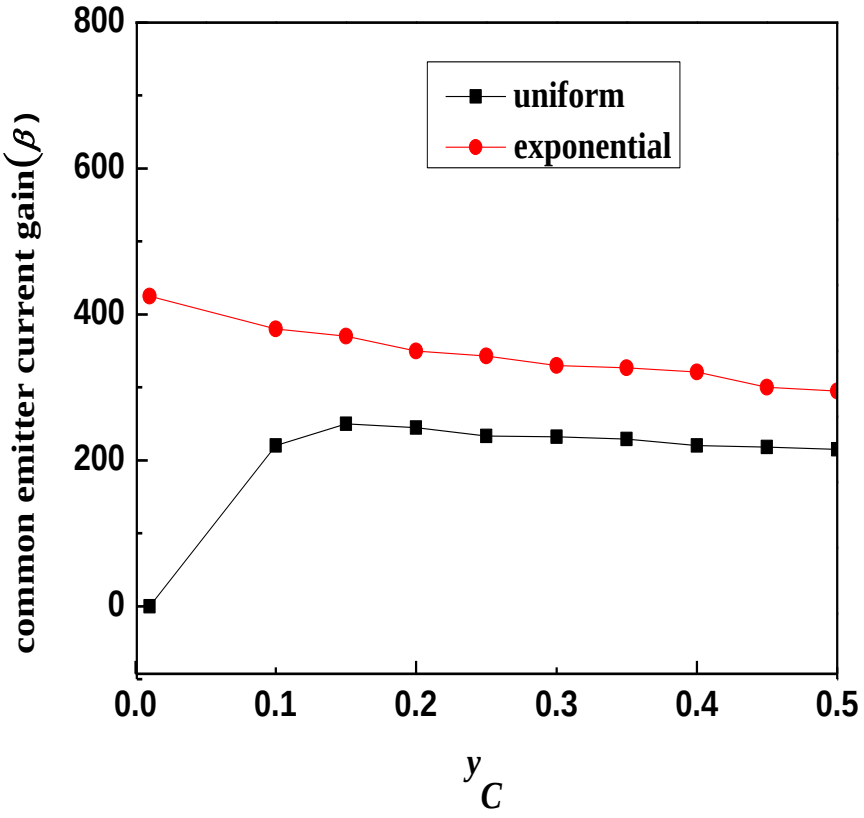

Figure 4.9: Common emitter current gain (β) for y_E=.2 and varying y_C for uniform and exponential base doping. J_{BO} is considered 7 pA/cm$^{2.}$

Table 4.1

Calculated value showing current gain and Early voltage for various y_C and y_E combination

In-mole fraction		Uniform base doping profile		Exponential base doping profile	
y_E	y_C	V_A	β	V_A	β
0.01	0.01	18	111	379	39
0.01	0.14	92	111	1937	29
0.01	0.25	980	85	17446	24
0.14	0.01	10	239	88	355
0.14	0.14	15	884	378	256
0.14	0.25	137	748	2880	202
0.25	0.01	15	240	-30	3551
0.25	0.14	6	3112	122	3339
0.25	0.25	15	378	378	2618

Table 4.1 shows calculated value of V_A and β for different devices. Here J_{BO} is considered 7 pA/cm^2.W_B=500Å.N_B (0) =10^{19} cm^{-3} and N_B (W_B) =10^{17} cm^{-3} for exponential and 10^{19} cm^{-3} is for uniform doped base.

4.3 CONCLUSION:

Determination of the effects of various parameters on Early voltage (V_A) and common emitter current gain *(β)* were obtained from the analytical expression derived in chapter 3. Here it can be observed that V_A and β is higly observed on In-mole fraction. Electron velocity saturation effect *(v_S)* was observed on diffusivity and collector current density *(J_{CO}).* It can be found that v_S have significant impact on both J_{CO} and diffusivity for uniform and exponential base doping profiles.

CHAPTER 5

CONCLUSION AND SUGGESIONS

5.1 CONCLUSION

Closed form analytical model were derived for early voltage *(V_A)* and common emitter current gain *(β)* for uniform and exponential base doping profiles with trapezoidal/triangular/box Indium profiles heterojunction bipolar transistor (HBT). In this model some effects were considered. Those effects field dependent mobility, doping dependent mobility, band gap narrowing (BGN) (due to both heavy doping and presence of Indium content in the base). Velocity saturation effects were also considered in this model. The effects of base doping profile and indium profile on V_A and β were observed in this work. Effects of Indium mole fraction on diffusivity *($D_{nInGaAs}$),* effective intrinsic carrier concentration *($n_{ieInGaAs}$)* and electric field *($E_{lInGaAs}$)* were studied. Electron velocity saturation $(v_s)$was studied on diffusivity and collector saturation crrent density *(J_{CO}).* It can be observed that (v_s) has significant impact on both J_{CO} and diffusivity for both uniform and exponential base doping profiles. The results obtained by using this analytical model compared with the results available in the previous work and found in good agreement.

5.2 SUGGESION FOR FUTURE WORK

Two different base doping profiles (uniform and exponential) with arbitrary Indium profiles were considered in this work. Analytical modeling of Early voltage *(V_A)* and common emitter current gain *(β)* were derived for uniform and base doping profiles considering field dependent mobility, doping dependent mobility, band gap narrowing and velocity saturation effect. Band gap narrowing (BGN) is considered due to heavy

doping and presence of Indium .the variation of V_A and β for uniform and exponential base doping profiles and indium profiles were addressed.

The HBT here was a *InGaAs* heterojunction bipolar transistor attempt should be taken to investigate Early voltage *(V_A)* and current gain (β) using this model for *InP, AlGaAs* etc.

Recombination effect is neglected in this analysis. Attempt should be taken to consider this effect on V_A and β.

This analysis is valid for low and moderate injection of minority carrier in the base. For high injection this model need to be changed.

Distortion of energy band at base-emitter and base-collector junction due to band gap engineering need to be considered, which will make possible more accurate result of V_A and β.

REFERENCES

[1] R.C. Jaeger and T.N. Blalock (2004). Microelectronic Circuit Design. McGraw-Hill Professional. p. 317. ISBN 0-07-250503-6

[2] Massimo Alioto and and Gaetano palumbo (2005). Moel and design of Bipolar and Mos current-Mode logic:CML,ECL and SCL digital Circuits.Springer.ISBN 1-4020-2878-4

[3] Paolo Antognetti and Giuseppe Massobrio (1993). Semiconductor Device Modeling with Spice. McGraw-Hill Professional. ISBN 0-07-134955-3.

[4] Orcad PSpice Reference Manual named PSpcRef.pdf, p. 209. This manual is included with the free version of Orcad PSpice, but they do not maintain a copy on line. If the link given here expires, try Googling PSpcRef.pdf.

[5] S. Y. Chiuand A. F. M.Anwar, "Effect of surface recombina-tion on the Early voltage in HBTs", Semicond. Sci. Technol, Vol. 14, No. 9, September 1999

[6] Y. D.Wang,X. Yang and H. W.Zhang, "Effect of Base Structure Optimization of SiGe HBTs on Early Voltage", In-stitute of Microelectronics, Tsinghua University,Beijing 100084,P.R.China, 2006.

[7] J.Ningyue and M.Zhenqiang, "Current gain of SiGe HBTs under high base doping concentrations",Semicond. Sci. Technol, Vol. 22, No. 1, January 2007.

[8] E. J. Prinz and J. C. Sturm, "Current Gain-Early Voltage-Products in Heterojunction Bipolar Transistors with Non-uniform Base Bandgaps", IEEE Electron Device Letters, Vol. 12, No. 12, December 1991

[9] J. S. Yuan and J.Song, "Early voltage of SiGe Heterojunction Bipolar Transistor", Electron Devices Meeting, IEEE Hon-kong, pp. 102-105, 1997.

[10] C. J. Eduardo and F. P.Cortes, "Early Voltage and Saturation Voltage Improvement in Deep Sub-Micron Technologies Using Associations of Transistors", SBCCI 08, September 1-4, 2008, Gramado Brazil

[11] M. Domeij and H. S.Lee, "High Current Gain Silicon Carbide Bipolar Power Transistors", International Symposium on Power Semiconductor Devices and IC's, Naples, Italy, June 4-8, 2006.

[12] M. J. Kumarand V.Parihar, "Surface Accumulation Layer Transistor (SALTran): A New Bipolar Transistor for En-hanced Current Gain and Reduced Hot-Carrier Degradation", IEEE transactions on Device and Materials Reliability, Vol. 4, No. 3, September 2004.

[13] V. S. Patri and M. J.Kumar, "Profile Design Considerations for minimizing base transit time in SiGe HBT's", IEEE Tran. on Electron Devices, Vol. 45, pp. 1725-1731, Aug 1998.

[14] A.Zareba, L. Łukasiak and A. Jakubowski, “The Influence of Selected Material and Transport Parameters on the Accuracy of Modeling Early Voltage in SiGe-Base HBT”, IEEE TransactionOnElectronDevices, Vol. 53, No. 8, August 2006.

[15] J.A.Babcock, L. J. Choi, A.Sadovnikov,W. V.Noort, C.Estonilo, P.Allard, S.Ruby and G.Cestra, “Temperature interaction of Early voltage, current gain and breakdown characteristics of npn and pnpSiGe HBTs on SOI” IEEE Bipolar/BiCMOS Circuits and Technology Meeting (BCTM), 2010.

[16] J.A.Babcock, A.Sadovnikov, L. J. Choi; W. V.Noort, P.Allard and G.Cestra,“Forward and inverse mode Early voltage dependence on current and temperature for advanced SiGe-pnp on SOI” IEEE Bipolar/BiCMOS Circuits and Technology Meeting (BCTM), 2011.

[17] X.Xiao-Bo,Z.He-Ming, H.Hui-Yong andT. Q.Jiang, “Early effect of SiGeheterojunction bipolar transistors” School of Microelectronics, Xidian University, Xi’an, Shaanxi, P. R China, 2012.

[18] http://www.pbs.org/transistor/album1/addlbios/egos.html

[19] R. G. Arns, "The other transistor: early history of the metal-oxide-semiconductor field-effect transistor," Engineering Science and Education Journal, vol. 7, pp. 233–240, October 1998

[20] W. Heywang and K. H. Zaininger, Silicon: The semiconductor material, evolution and future of a technology, Springer, 2004.

[21] C. M. Snowden and E. Snowden, Introduction to Semiconductor Device Modelling, 1 ed.: World Scientific Publishing Co, Singapore, 1998.

[22] S. M. Sze and K. K. Ng, Physics of Semiconductor Devices, 3rd ed. New Jersey: Jown Wiley & Sons, 2007

[23] B. G. Streetman, Solid State Electronic Devices, 4th ed.: Prentice Hall, 1995

[24] C. M. Grens, P. Cheng, and J. D. Cressler, "An Investigation of the Large-Signal RF Safe-Operating-Area on Aggressively-Biased Cascode SiGe HBTs for Power Amplifier Applications," 2009

[25] P. Asbeck, Handbook of Thin Film Devices vol. 1: Academic Press, 2000.

[26] B. Hughes, "A temperature noise model for extrinsic FET‟s," IEEE Trans. on Microwave Theory and Techniques, vol. 40, pp. 1821-1832, September 1992.

[27] W. Shockley: 'Circuit Element Utilizing Semiconductive Material', United States Patent 2,569,347, 1951.

[28] The phototransistor effect: "The Kroemer factor is a function of the physical parameters of the materials making up the heterojunction, and can be expressed in the following way [formula given]"

[29] R. A. Levy, Microelectronic Materials and Processes: Kluwer Academic Publisher, 1989.

[30] R.J.V.Overstraete, , H.J Deman,. and Mertens, R.P. , ‘’ Transport equation in heavy doped silicon’’. IEEE Trans . Electron Devices , vol .ED-20.pp 290-298, 1973.

[31] S. Mattisson, "Architecture and technology for multistandard transceivers," Proceedings of the Bipolar/BiCMOS Circuits and Technology Meeting (BCTM), pp. 82-85, September 2002.

[32] K. Suzuki , “Optimum base doping profile for minimum base transit time considering velocity saturation at base-collector junction and dependence of mobility and band gap narrowing on doping concentration”, IEEE tran. On Electron Devices, vol.48, pp.2102-2107,2001.

[33] K. Suzuki , “Optimum base doping profile for minimum base transit time “ IEEE tran. On Electron Devices, vol.38, pp.2128-2133,1991.

[34] L. Larson, "Integrated Circuit Technology Options for RFIC‟s - Present Status and Future Directions," IEEE Journal of Solid-State Circuits, vol. 33, pp. 387-399, March 1998.

[35] S. Mattisson, "Architecture and technology for multistandard transceivers," Proceedings of the Bipolar/BiCMOS Circuits and Technology Meeting (BCTM), pp. 82-85, September 2001.

[36] D. Y. C. Lie, J. Yota, W. Xia, A. B. Joshi, R. A. Williams, R. Zwingman, L. Chung, and D. L. Kwong, "New experimental findings on process-induced hot-carrier degradation of deep-submicron N-MOSFETs," IEEE International Reliability Physics Symposium, pp. 362-369, March 1999.

[37] D. Y. C. Lie, X. Yuan, L. E. Larson, Y. H. Wang, A. Senior, and J. Mecke, ""RF-SoC": low-power single-chip radio design using Si/SiGe BiCMOS technology," Proceedings of the 3rd International Microwave and MillimeterWave Technology, pp. 30-37, August 2002.

[38] X. Yuan, D. Y. C. Lie, L. E. Larson, J. Blonski, J. Gross, M. Kumar, J. Mecke, A. Senior, Y. Chen, A. Pho, and D. Harame, "RF linearity study of SiGe HBTs for low power RFIC design I," Proceedings of the 3rd International Microwave and Millimeter Wave Technology, pp. 70-73, August 2002.

[39] Z. Xu, G. Niu, L. Luo, P. S. Chakraborty, P. Cheng, D. Thomas, and J. D. Cressler, "Cryogenic RF Small-Signal Modeling and Parameter Extraction of SiGe HBTs," IEEE Topical Meeting on Silicon Monolithic Integrated Circuits in RF Systems, SiRF'09, pp. 1-4, Jan 2009.

[40] K. H. Kwok and C. R. Selvakumar, "Profile design considerations for minimizing base transit time in SiGe HBTs for all levels of Injection before onset of Kirk effect," IEEE Trans. on Electron Devices, vol. 48, pp. 1540-1549, 2001

[41] J. S. Yuan, "Effect of base profile on the base transit time of the bipolar transistor for all levels of injection," IEEE Trans. on Electron Devices, vol. 41, pp. 212-216, Feb 1994.

[42] L. Larson, "Integrated Circuit Technology Options for RFIC‟s - Present Status and Future Directions," IEEE Journal of Solid-State Circuits, vol. 33, pp. 387-399, March 1998.

[43] A.Zareba, L. Lukasiak, and A. Jakubowski, "Modeling of SiGe-base heterojunction bipolar transistor with gaussian doping distribution," Solid-State Electronics, vol. 45, pp. 2029-2032, 2001.

[44] http://scitation.aip.org/content/aip/journal/jap/40/9/10.1063/1.1658265

[45] D. A. Neamen, Semiconductor Physics and Devices: Basic Principles, 3rd ed. New York: McGraw-Hill, 2003.

[46] R. Muller and T. Kamins, Device electronics for intregrated circuits, 2nd ed. New York: Wiley, 1986.

[47] S. Basu, "Analytical modelling of base transit time of SiGe HBTs including effect of temperature," International Semiconductor Conference, CAS'08, vol. 2, pp. 339-342, Oct 2008.

[48] S. T. Chang, C. W. Liu, and S. C. Lu, "Base transit time of graded-base Si/SiGe HBTs considering recombination lifetime and velocity saturation," Solid-State Electronics, vol. 48, pp. 207–215, 2004.

[49] B. Y. Chen and J. B. Kuo, "An accurate knee current model considering quasi-saturation for BJTs operating at high current density," Solid-State Electronics, vol. 38, pp. 1282–1284, Jun 1995

[50] J. d. Alamo , "Simultaneous measurement of hole lifetime, hole mobility and bandgap narrowing in heavily doped n-type silicon," IEDM Tech. Dig., pp. 290-293, 1985.

[51] S. Swirhum, and R. M. Swanson, "Simultaneous measurement of hole lifetime, hole mobility and bandgap narrowing in heavily doped n-type silicon," IEDM Tech. Dig., pp. 290-293, 1986.

[52] J. W. Slotboom and H. C. d. Graaff, "Measurement of bandgap narrowing in Si bipolar transistors," Solid-State Electronics, vol. 19, pp. 857–862, 1976.

[53] T. C. Lu and J. B. Kuo, "A closed form analytical BJT forward transit time model considering bandgap narrowing effects and concentration dependent diffusion coefficients," Solid-State Electronics, vol. 35, pp. 1374–1377, 1992.

[54] H. Kroemer, "Two integral relations pertaining to electron transport through a bipolar transistor with a nonuniform energy gap in the base region," Solid-State Electronics, vol. 28, pp. 1101–1103, 1985.

[55] K. Suzuki and N. Nakayama , “Base transit time of shallow-base bipolar transistors considering velocity saturation at base-collector junction IEEE trans.Electron device,ED-16, 1969.

[56] S.D Tyagi, K. Singh , S.K. Ghandhi; J.M Borrego,. "Photovoltaic Specialists Conference, 1991., Conference Record of the Twenty Second IEEE

[57] Fazle Rabbi, Yeasir Arafat, M. Ziaur Rahman Khan, "The Early Voltage and current gain of $Si_{1-y}Ge_y$ Heterojunction Bipolar Transistor"

APPENDIX

DERIVATION FOR LOW AND MODERATE INJECTION

1. $-J_n(x) = qD_n(x)\frac{dn\,(x)}{dx} + q\mu_n(x)n(x)E(x)$ …. (3.4a)

$J_p(x) = -qD_p(x)\frac{dp\,(x)}{dx} + q\mu_p(x)p(x)E(x)$ …. (3.4b)

Where $J_c(x) = J_n(x) + J_p(x)$ ….(3.5)

2. $E(x) = V_T\ \frac{d}{dx}[\ln\left(\frac{\mathrm{p\,(x)}}{\mathrm{n_{ie}^2(x)}}\right)]$ …. (3.7a)

Therefore $E(x) = V_T(\frac{1}{p(x)}\frac{dp(x)}{dx} - \frac{1}{n_{ie}^2(x)}\frac{dn_{ie}^2(x)}{dx})$ …. (3.7b)

3. $N_B(x) = N_B(0)$ …. (3.11a)

$N_B(x) = N_B(0)$ …. (3.11b)

Where $m_{exp} = \frac{\ln(N_B(0)/\,N_B(W_B)\,)}{W_B}$ …. (3.12)

$N_B(0)$ And $N_B(W_B)$ is the peak base doping concentration at the base-emitter and base-collector junction respectively.

4. $D_{nGaAs}(x) = D_n$ …. (3.13a)

$D_{nGaAs}(x) = D_n e^{m_{1\,exp}x}$ …. (3.13b)

Where $D_n = D_{no}\left(\frac{N_B(0)}{N_r}\right)^{-\gamma_1}$, $D_{no} = 103.6\ \frac{cm^2}{s}$, $N_r = 10^{17}cm^{-3}$

$m_{1\,exp} = m_{exp}\gamma_1$ and $\gamma_1 = 0.43$.

5. $D_{nInGaAs}(x) = b\ D_{nGaAs}(x)$ …. (3.14a)

Where, b=1+3y_{av}.

6. $V_{sA} = c\ v_s$ …. (3.14b)

Where, c=0.342/ [0.342+y_{av} (1-y_{av})] and v_s=1.4×10^7 cm/s

7. $(|E|, x) = \frac{V_s}{a|E| + E_{cGaAs}(x)}$ .... (3.15a)

Where, a=0.7743

$E_{cGaAs}(x) = \frac{V_s}{\mu_{nGaAs}(x)}$ .... (3.15b)

8. $n^2_{ieInGaAs}(x) = \gamma(x) n^2_{ioGaAs} e^{\frac{\Delta E_{geff}(x)}{KT}}$ ..... (3.16a)

Where, n_{ioGaAs}=1.79x10^6 cm^{-3}

$\gamma(x) = \exp[-\sqrt{5y(x)}]$ .... (3.16b)

9. $p_l(x) = n_l(x) + N_B(x) \approx N_B(x)$ .....(3.10)

10.$\Delta E_{geff}(x) = \Delta E_{gHD}(x) + \Delta E_{gIn}(x)$ .... (3.16d)

Where $\Delta E_{gHD}(x) = q V_{gHD} \ln\left(\frac{N_B(x)}{N_r}\right)$ .... (3.16e)

V_{gHD}=18 mV

11. $\Delta E_{gIn}(x) = q V_{gIn} y(x)$ .... (3.16f)

V_{gIn} =750 mV.

12. $n^2_{ieInGaAs}(x) = n^2_{ioGaAs} e^{\gamma_3 \gamma_e} \left(\frac{N_B(0)}{N_r}\right)^{\gamma_2} e^{(m_3 x - m_2 x^a)} . \gamma(x)$..(3.16g) (using 3.16a-3.16f)

Where, $\gamma_2 = {V_{gHD}}/{V_T} = 0.69, \gamma_3 = {V_{gGe}}/{V_T} = 28.84, m_3 = \gamma_3 . m_{In}$

13. $E_{lInGaAs}(x) = V_T \left(\frac{1}{N_B(x)} \frac{dN_B(x)}{dx} - \frac{1}{n^2_{ieInGaAs}(x)} \frac{dn^2_{ieInGaAs}(x)}{dx}\right)$ .... (3.17a)

Using 3.11(a,b),(3.16g) and (3.17a),electric field under low injection will be:

14. $E_{lInGaAs}(x) = V_T \left(m_3 + 0.31\alpha m x^{(\alpha-1)} - \left(\frac{m_{In}\sqrt{5}}{2}\right)\frac{1}{\sqrt{m_{In}x+y_E}}\right)$ … (3.17b)

(Using 3.11(a,b),(3.16g) and (3.17a))

m= 0 for uniform and $m_{exp}.y_2$ for exponential

15. $J_C = J_{CO}\, e^{(\frac{qV_{BE}}{kT})} = \frac{qe^{(\frac{qV_{BE}}{kT})}}{\int_0^{W_B}\frac{N_B(x)}{n^2_{ieInGaAs}(x)D_{nSiGe(x)}}dx + \frac{N_B(W_B)}{n^2_{ieInGaAs}(W_B)v_{sA}}}$ …. (3.18a)

16. $\beta = \frac{J_{CO}}{J_{BO}} = \frac{\frac{q}{J_{BO}}}{\int_0^{W_B}\frac{N_B(x)}{n^2_{ieInGaAs}(x)D_{nInGaAs(x)}}dx + \frac{N_B(W_B)}{n^2_{ieInGaAs}(W_B)v_{sA}}}$ …. (3.18b)

17. $V_A = J_C\left(\frac{\delta W_B}{\delta J_C}\frac{\delta V_{BC}}{\delta W_B}\right)V_{BE} = constant$ (3.19a)

Furthermore

$$V_A = \frac{qn^2_{ieInGaAs}(W_B)D_{nInGaAs}(W_B)}{C_{BC}} \times \left(\int_0^{W_B}\frac{N_B(x)}{n^2_{ieInGaAs}(x)D_{nInGaAs(x)}}dx + \frac{N_B(W_B)}{n^2_{ieInGaAs}(W_B)v_{sA}}\right)$$

…..(3.19b

18. $\beta V_A = \frac{q^2 n^2_{ieInGaAs}(W_B)D_{nInGaAs}(W_B)}{J_{BO}C_{BC}}$ …… (3.19c)

19. $n^2_{ieInGaAs}(x) = n^2_{ieSiGe}InGaAs(0).e^{(m_3x - m_2x^a)}$ …… (3.20)

Where $n^2_{ieInGaAs}(0) = n^2_{ioGaAs}e^{\gamma_3 y_e}(N_B(0)/N_r)^{y2}.y_r$

$E_{lInGaAs}(x) = V_T\,(m_3 + .31\alpha m x^{\alpha-1})$ …. (3.21)

20. $V_A = (I_1 + \frac{N_B\,(W_B)}{n^2_{ieInGaAs.}v_{sA}})(\frac{qn^2_{ieInGaAs}(W_B)}{c})(\frac{bv_sD_n\,e^{m_1W_B}}{V_s + am_{032}D_n\,e^{m_1W_B}})$ (3.22)

Where

$$I_1 = \frac{N_B\,(0)\; a\; m_{032}}{n^2_{ieInGaAs}(0) b v_s\; m_{132}}\left(1 - e^{-m_{132}W_B}\right) + \frac{N_B(0)}{n^2_{ieInGaAs}(0) b D_n m_{0132}}\left(1 - e^{-m_{0132}W_B}\right)$$

And $m_{32} = m_3 - m_2$, $m_{032} = m + m_3 - m_2$, $m_{132} = m_1 + m_{32}$, $m_{0132} = m + m_1 + m_{32}$.

21. For exponential base doping profile can be found by the expression given below:

$$\beta = \frac{J_{CO}}{J_{BO}} = \frac{{}^{q}/_{J_{BO}}}{I_1 + \frac{N_B(W_B)}{n^2_{ieInGaAs}(W_B) v_{SA}}} \tag{3.24}$$

22. For uniform base doping profile,

$$V_A = \left(I_2 + \frac{N_B\,(0)}{n^2_{ieInGaAs.} v_{sA}}\right)\left(\frac{q n^2_{ieInGaAs}(W_B)}{c}\right)\left(\frac{b v_s D_n}{a m_3 D_n + V_s}\right) \tag{3.25}$$

Where

$$I_2 = \frac{N_B\,(0)(a m_3 D_n + V_s)}{n^2_{ieInGaAs}(0) b v_s D_n\, m_3}\left(1 - e^{-m_3 W_B}\right) \tag{3.26}$$

23. For uniform base doping profile can be found by the expression given below:

$$\beta = \frac{J_{CO}}{J_{BO}} = \frac{{}^{q}/_{J_{BO}}}{I_2 + \frac{N_B(W_B)}{n^2_{ieInGaAs}(W_B) v_{SA}}} \tag{3.27}$$